FINAL REPORT, PHASE I

ATOMIC HYDROGEN MASER FOR SPACE VEHICLE APPLICATION

April 1968

Contract NASW-1337

(March 1, 1966 to March 31, 1968)

Prepared by

HEWLETT hp PACKARD

Frequency and Time Division-East, Salem Road, Beverly, Massachusetts

for

NATIONAL AERONAUTICS AND SPACE ADMINISTRATION

Office of Space Science and Applications

Washington, D.C. 20546

GPO PRICE $ _____

CFSTI PRICE(S) $ _____

Hard copy (HC) 3.00

Microfiche (MF) .65

ff 653 July 65

Final Report -- Phase I

Research Leading to the Development of an ATOMIC HYDROGEN MASER FOR SPACE VEHICLE APPLICATION

April 1968

Contract NASW-1337

Period Covered:
March 1, 1966 to March 31, 1968

Prepared by:
R. F. C. Vessot and M. W. Levine

HEWLETT-PACKARD Co.
Frequency and Time Division - East
Beverly, Massachusetts

for

NATIONAL AERONAUTICS AND SPACE ADMINISTRATION
Office of Space Science and Applications
Washington, D.C.

Foreword

The discussion that follows is the first formal report to NASA on Contract NASW-1337 and covers over two years of work in this laboratory on the first phase of a program to develop a satellite clock for use in a relativistic red shift experiment. Since the report may receive distribution among those unfamiliar with the over-all objectives of the program, this review and outline are provided.

The atomic hydrogen maser, first operated by Ramsey, Kleppner and Goldenberg at Harvard in 1960, was developed as a commercial laboratory instrument by the Beverly, Mass., group now constituting Hewlett-Packard's Frequency and Time Division - East. Because of the maser's extremely high precision and long term stability exceeding that of any other known device, the Beverly and Harvard groups proposed it as a space-borne clock which, measured against a ground-based clock, could be used to test the so-called "red shift" or effect of gravity on time predicted in Einstein's General Theory of Relativity. Such measurements would exceed in accuracy by one to two orders of magnitude the ground-based measurements of Pound[1] involving the Mössbauer effect and could be expected to reinforce his findings in support of Einstein's theory. Techniques developed could contribute to other future applications, including space exploration with precise clocks to test physical phenomena such as possible mass asymmetries of the universe, as well as demonstrating the feasibility of the use of a satellite for navigation and the distribution of accurate time signals.

Accordingly, the two groups presented proposals to NASA in early 1965 which resulted in award of the subject contract NASW-1337 issued by NASA Headquarters for development of a hydrogen maser for space applications; the Harvard group was awarded a two-year grant, NRG22-07-054, for theoretical studies on maser improvement for these goals, both programs under the over-all technical direction of Professor N. F. Ramsey of Harvard. The final

[1] R. V. Pound and J.L. Snider, Phys. Rev. Letters 13, 539 (1964).

experiment is expected to involve NASA's Marshall Space Flight Center and Manned Spacecraft Center and will be accomplished by placing two or three hydrogen masers on a manned spacecraft in earth-synchronous orbit, at about 22,300 miles above the earth, for a period of at least two weeks, and comparing their clock rates by telemetry with those of ground-based hydrogen masers. Theory predicts that the space clocks will gain 46.5 microseconds per day with respect to the ground clocks. The data will also be analyzed for a possible periodic daily variation in the apparent rates of the clocks, which could arise either from a dependence of the rate of a clock upon motion relative to the fixed stars or from a variation of the velocity of light with direction. In this respect the proposed experiment should be 30 times more sensitive than the best previous test by Turner and Hill. [2]

It may be noted in passing that, among several other current programs aimed at testing Einstein's general or special theories of relativity,[3] Hewlett-Packard's atomic hydrogen maser is playing a role in another approach. Installed at M.I.T.'s Haystack antenna, a maser is part of equipment being used to measure the effect of solar gravity in slowing down radar impulses beamed to Venus as it passes behind the sun. These studies[4] should eventually help to reinforce Einstein's theory or the more recent Dicke-Brans concept. Other current applications of the maser's unique properties include its use in radio astronomy for long-baseline interferometer experiments.

Following, then, is an account of the first phase in the design and development at Hewlett-Packard's laboratories in Beverly of the hydrogen maser that will be mounted, with its accompanying electronics, and orbited in a spacecraft to provide measurements heretofore unattainable.

---

[2] K. C. Turner and H. A. Hill, Phys. Rev. 134, B252 (1964).

[3] W. Sullivan, "Einstein's Theory Now Put to the Test," N.Y. Times, March 3, 1968 (p. 8E).

[4] I. I. Shapiro, IEEE Spectrum 5, No. 3, p. 70 (1968).

TABLE OF CONTENTS

TABLE OF FIGURES

I. INTRODUCTION

Work began on the laboratory prototype model of the satellite maser on March 1, 1966. At the outset it was decided to divide the effort into two categories--mechanical and electronics--and this report will describe the progress in each of these areas, with some discussion of telemetry system requirements.

There were several important questions in mechanical design that had to be resolved in order to design a maser suitable for space use. Considerations of size, weight and power consumption are important and most important of all is the mechanical ruggedness and thermal stability of the maser oscillator itself. The program began with a study of cavity and magnetic field configurations for optimum accuracy of output frequency consistent with mechanical and thermal stability. A study was made of various compact configurations of magnetic shields and low field solenoids for the maser bulb region.

The question of maintaining a controlled cleanliness in the system led to a decision early in the program to use an on-board vacuum system rather than to rely on the dubious cleanliness of the space vacuum due to the possibility of outgassing from the spacecraft and jettisoning of low vapor pressure material. It was decided that s special ionization pump, using the Penning discharge principle as in conventional masers, would be used. This pump was designed in collaboration with Varian Associates' Vacuum Products Division with low power, small size, light weight and ease of magnetic shielding in mind. The pump has a nominal speed for air of about 200 liters/sec. For hydrogen, this number can be approximately doubled. The total capacity of the pump based on the area of the titanium anodes in the Penning discharge is comparable to that used in the H-10 masers and these have operated in excess of two years without pump element replacement. The weight of the pump is due mostly to the permanent Alnico magnets and the soft iron pieces that complete the magnetic circuit. It is very likely that this weight can be reduced considerably by using ceramic slab magnets and less massive iron pieces.

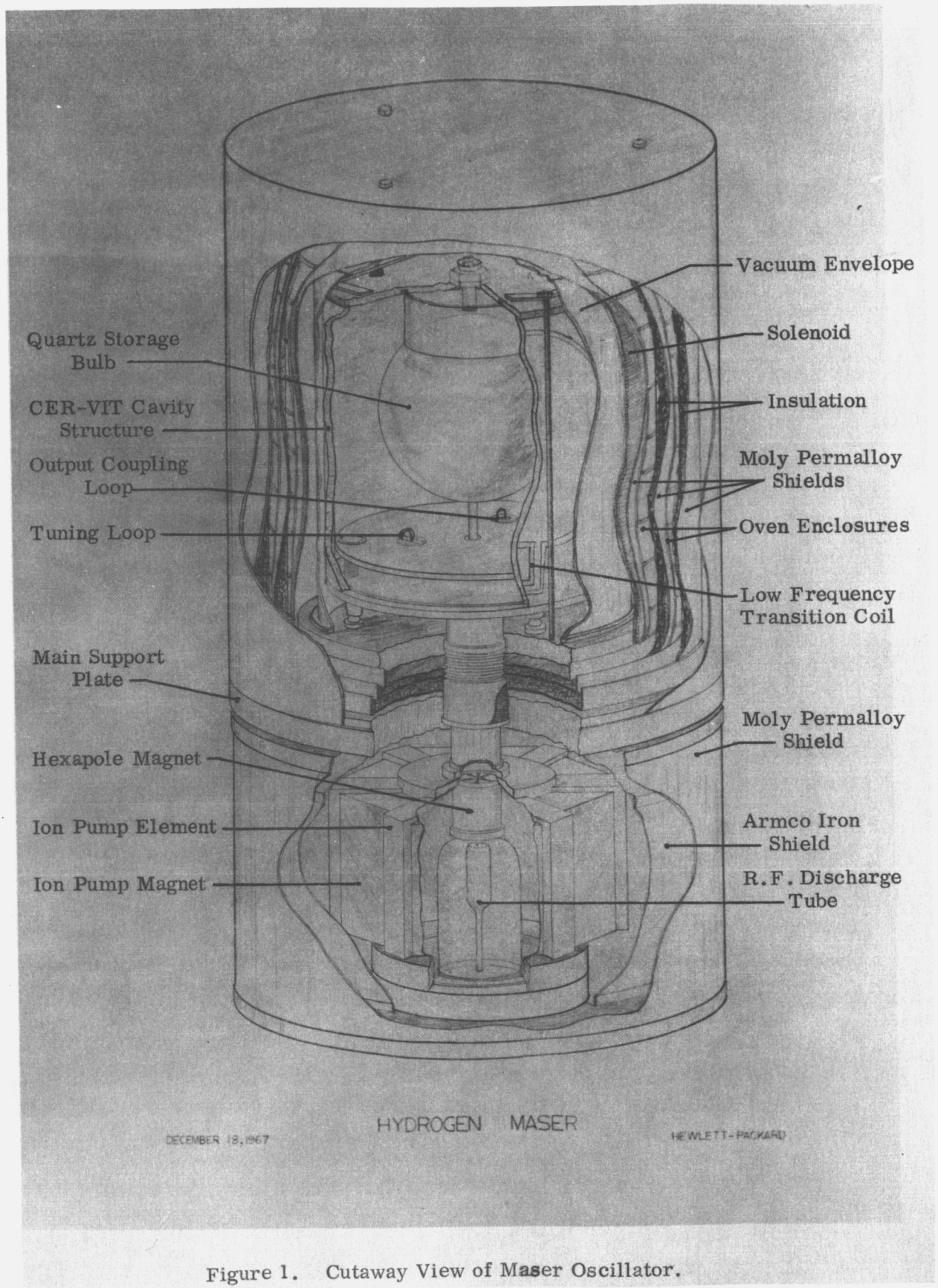

Figure 1. Cutaway View of Maser Oscillator.

The very important question of reliability of dissociator operation had to be studied and means other than the r.f. dissociator were studied for producing a beam of hydrogen atoms. This program has also been continued as part of a Hewlett-Packard effort for obtaining a reliable dissociator.

A cut-away drawing of the maser oscillator is shown in Figure 1.

Systems for telemetering the rate of the satellite clock were studied. A two-way doppler cancelling system was conceived. This system was analyzed including first and second order doppler effects and the gravitatonal effect on the telemetry signals. The analysis shows that it is possible, by phase coherent telemetry techniques, virtually to eliminate all sources of error in the propagation and to obtain a beat signal at the ground station and on the satellite that includes only the gravitational effects and the second order doppler effects due to the relative velocities and gravitational potentials of the two clocks.

This data is available both on the ground and in the satellite and it is important to have both in order to anticipate the question of there being a lack of reciprocity in the telemetry link.

A block diagram has been made of a system using telemetry channels associated with the unified S-band system. Other telemetry and command signals for operating the experiment can be transmitted using subcarrier sidebands on the phase coherent clock signals.

The electronics system for keeping the cavity resonance frequency at the resonance frequency of the atom in the bulb and the system for converting the frequency of the maser to a usable frequency at a useful level had already been conceived prior to the beginning of this program; however, much work remained to be done to make an operating system for testing the cavity tuning system. Since some previous experience in frequency synthesizing and phase locking techniques existed, it was possible to build a prototype breadboard without a great deal of experimentation.

Circuits for controlling pressure and temperature have been made for other masers, and electronics system studies were made to perform these control

functions as efficiently as possible. Thermal and other environmental specifications, due to uncertainty in the spacecraft configuration , have been somewhat vague and have led to a hold-up in this phase of the effort. Since the techniques involved are fairly standard and do not involve any advance in present technology, it was considered wise not to press this development until firmer specifications are available.

II. MECHANICAL DESIGN

A. GENERAL CONSIDERATIONS

The first iteration of design effort has been made for a small maser oscillator with the following characteristics:

Overall height	32 inches
Overall cylindrical diameter	18 inches
Overall weight	300 pounds

The breakdown of weight is as follows.

Item	Weight in lbs.	% of Total Weight
Cavity assembly	20	6.7
Vacuum envelope	25.5	8.5
VacIon® pump	90	30.0
Cavity magnetic shields	49.5	16.5
Pump magnetic shields	35.0	11.7
Dissociator	15	5.0
Miscellaneous hardware, ovens, solenoid, etc.	65	21.6
	300 lbs.	100 %

The mechanical design must be closely associated with thermal design. The most exacting part of the design is that of the cavity, which should not be detuned more than 100 Hz. as a result of the mechanical and acoustic vibrations during launch. Further, the mounting system must permit good thermal isolation of the cavity so that the temperature gradients are small, allowing full utilization of the passive thermal compensation of the cavity design.

Magnetic shields surrounding the cavity-bulb assembly are required to keep the spurious fields from the ion pump and other fields from the bulb region. These shields contribute substantially to the weight and in this first iteration of design their thickness was made equal to that of presently used shields. The

®Varian Associates.

significance of the configuration is important and the question of shield thickness and weight reduction can be answered later. From calculations of flux density it appears that the two inner shields can be substantially reduced in thickness without compromising shielding effectiveness.

It was decided to integrate the magnetic shields with the ovens and employ the space from the oven insulation as the separation between the magnetic shields. In designing the shields and ovens and with an eye to reducing the weight of the inner magnetic shields, the aluminum oven heater supports also support the magnetic shields. To prevent magnetic leakage, the magnetic shields should have few and relatively small-sized openings. The thermal enclosure also should be as closed as possible. Structural supports to hold the cavity should have small cross section, low thermal conductivity, and also be of small diameter so as to penetrate through the ovens and shields without compromising the effectiveness of the ovens and the shields.

The vacuum connection from the main pump to the bell jar system enclosing the cavity must have sufficient pumping speed and yet not have an excessively large cross section.

B. CAVITY-BULB STRUCTURE DESIGN

The design for the cavity-bulb structure is shown in Figure 2. The cavity material is fused silica. The bulb is 7 inches in diameter, which is nearly the size for the optimum spherical filling factor. The bulb is made of clear fused silica and is mounted by a fused silica skirt to the top plate of the cavity. This gives a low aspect ratio mounting structure and supports the thin-walled bulb in a uniform way near its line of greatest diameter. The joint to the plate is made using epoxy cement in a groove cut so as to minimize any possible lossy interaction with electric r.f. fields. The cavity cylinder, also made of fused silica, is mounted on a ring at its base, which in turn is connected to the aluminum bell jar base plate via a three-ball kinematic mount made of alumina balls and cones as shown in the figure. The cavity assembly is held to the bell jar base plate by pressure applied by six springs connected to an articulated linkage at the top

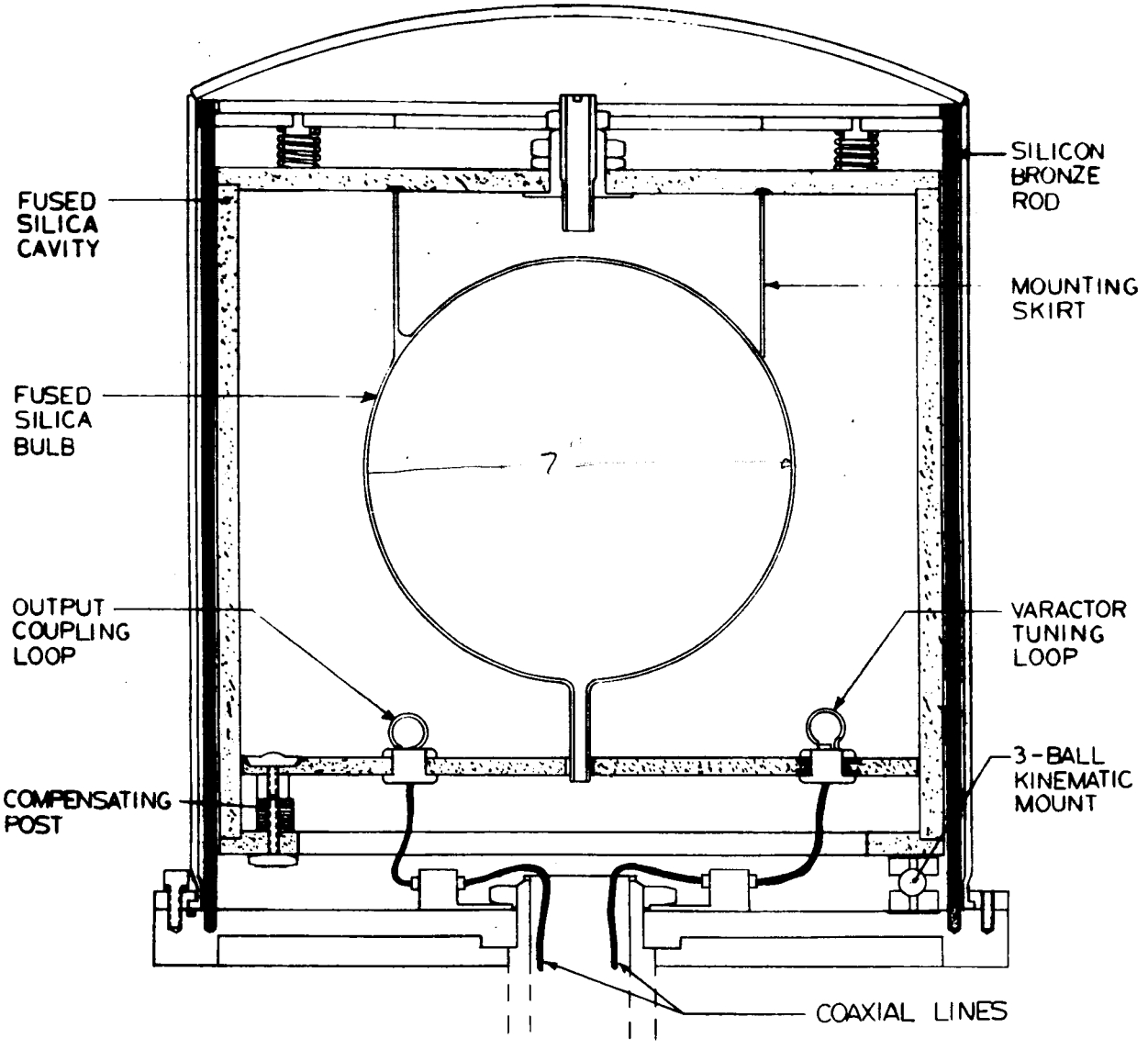

HYDROGEN MASER CAVITY STRUCTURE

Figure 2.

of the cavity to distribute the load. Six silicon bronze rods connect the linkage to the bell jar base and the tension in these is adjusted to obtain the desired pre-load stress to hold the cavity to the plate. Thermal expansion in the quartz cylinder is compensated by thermal expansion in three magnesium alloy posts that support the bottom plate of the cavity to the mounting ring. The length and coefficient of expansion of the material of the posts is chosen to provide a tuning rate with temperature equal and opposite in sign to the thermal cavity tuning rate of the cavity cylinder.

Stresses due to the difference in radial thermal expansion between the aluminum base plate and the quartz are largely absorbed by the kinematic mount. The residual radial stress applied via the mounting ring to the cavity cylinder dies out rapidly with axial distance along the cavity.

The bulb is equipped with an integral collimator; the interior of the bulb and the collimator tube is coated with F.E.P. Teflon.

Tuning of the cavity is accomplished in three stages. Coarse tuning is obtained by using metal shims beneath the compensating posts. The tuning rate is approximately 30 kilocycles per 0.001 inch. Finer tuning is done in two ways--electronically by a loop-coupled variable capacitor (varactor) in the interior of the cavity, and by a mechanical tuning plunger at the top of the cavity whose function is to permit adjustment of the cavity resonance frequency to the center of the electronic tuning range. The tuning loop is mounted to the base plate and can be rotated so as to vary the coupling with the r.f. magnetic field and thus vary its effective tuning range. The tuning range is adjusted so that the cavity is tuned over 10 kHz with a voltage range from 1 V to 8 V applied to the varactor.

The maser output signal is obtained from a coupling loop in the maser cavity which is connected through the vacuum envelope by a coaxial cable. A similar coaxial line is used to apply the tuning diode voltage.

The fused silica cavity has a highly conductive inner surface of silver applied from a silver-glass frit mixture that is painted and sintered at 670°C. The surface obtained in this way is burnished to compress the porous silver surface and

improve the conductivity. An unloaded cavity Q of 50,000 is obtained in the cavity-bulb structure. The low frequency coil for inducing the field dependent atomic transitions used for measuring the magnetic field is made by applying silver to the exterior of the cavity in a two-turn loop configuration so as to provide an oscillating magnetic field transverse to the axis of the cavity. The signal is applied to the coil through a third coaxial line. Care has been taken in this design to avoid conducting loops where thermoelectric currents can create unwanted magnetic fields. The cavity itself is grounded only through the r.f. output line. The diode tuning loop assembly is not connected to the inner conductive surface of the cavity. The same is true of the low frequency coil.

C. VACUUM ENVELOPE

As shown in Figure 3, the vacuum system consists of two chambers connected by a neck tube 2 inches in diameter and $3\frac{1}{2}$ inches long. The upper chamber containing the cavity-bulb assembly is made of nonmagnetic material (aluminum) and is thermally isolated from the outside of the maser by using thin-walled silicon bronze bellows for the neck tube and $\frac{1}{4}$-inch diameter titanium studs for mechanical support. The lower chamber consists of the pump structure and encloses the hexapole state selecting magnet and r.f. dissociator assembly. The pump, which has been specially designed for the satellite maser, uses six pumping elements in an array that permits a closed magnetic circuit that is relatively easy to shield. The core of the pump is a cylinder $5\frac{3}{4}$ inches in diameter, and 45 per cent of the wall area is taken by the six pumping element ports.

D. MAGNETIC SHIELDS AND SOLENOID

Both vacuum chambers are enclosed in magnetic shields. The upper chamber is enclosed in a concentric set of molybdenum-permalloy magnetic shields that also includes a two-stage oven for thermal control of the cavity. The lower chamber is enclosed by a double layer of magnetic shielding to prevent field leakage from the VacIon pump. All shields have end caps and these have the necessary holes for mounting fasteners and tubulation. The configuration of both sets of shields is shown in Figure 3.

Fig. 3. Schematic View of Maser Oscillator.

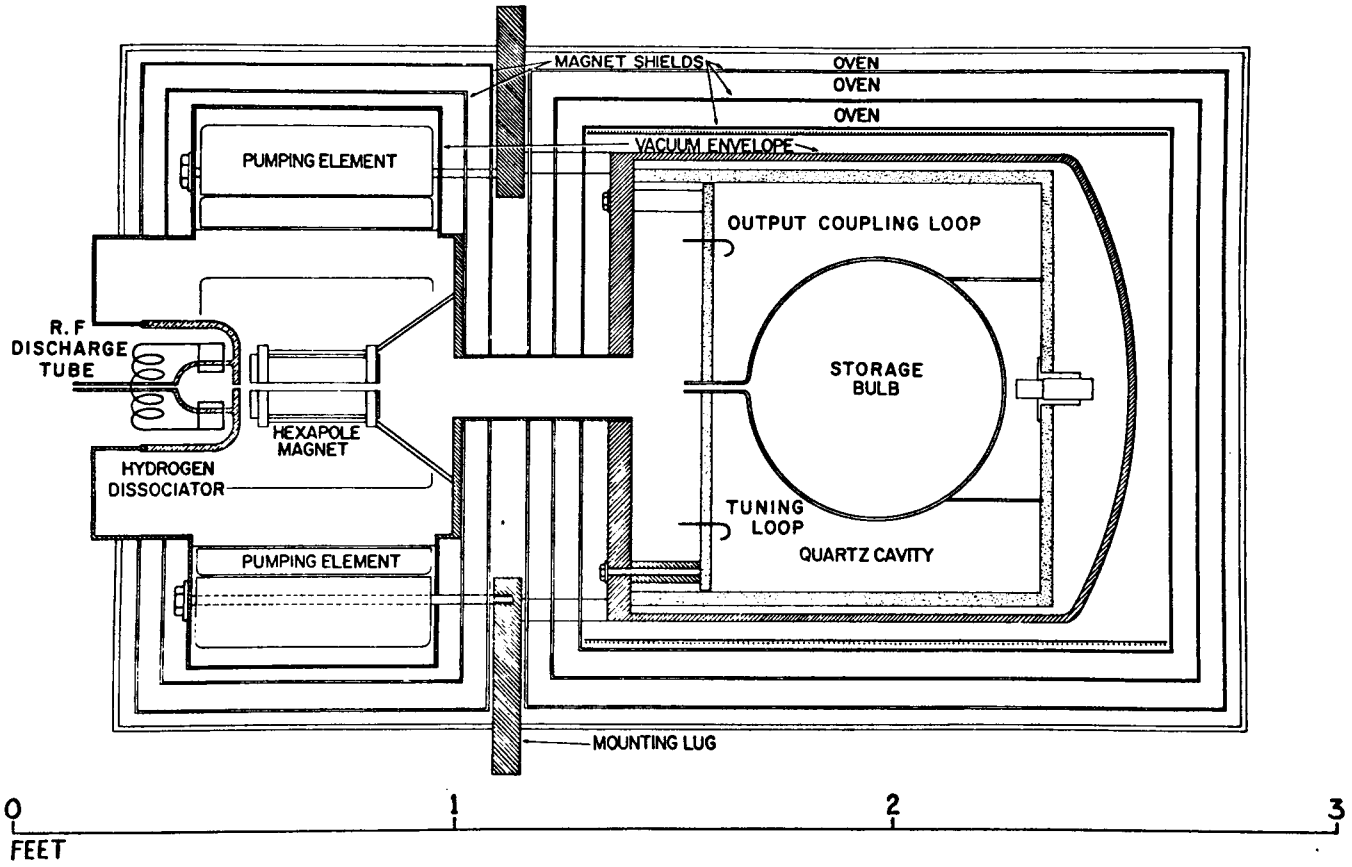

The solenoid that applies a uniform magnetic field to the bulb is located inside the innermost magnetic shield and is made to fit as closely as possible to the inner diameter of the shield cylinder. The coil is close-wound in two layers to cancel the fields from the go-and-return wires connecting to the coil. Three coil segments are used and these are laid out so as to provide corrections for end effects. A fourth coil, wound in the Helmholtz configuration, completes the design. This multiple-wound solenoid is discussed by Hanson and Pipkin in the Review of Scientific Instruments, Vol. 36, No. 2, February 19, 1965.

The magnetic shield, oven, cavity, solenoid assembly is held to the cavity base plate by three titanium rods running the length of the assembly and holding the three top end covers against the solenoid cylinders. Spacer bushings, made from a low thermal conductivity cross-linked polystyrene material, separate the shields.

E. THE R.F. DISCHARGE HYDROGEN DISSOCIATOR

As shown in Figure 3, the dissociator and state selector are located within the ion pump enclosure. The r.f. discharge used in the early prototype maser is similar to those used in the previous H-10 masers. The dimensions have been changed. The discharge tube, shown in the figure, measures $1\frac{1}{2}$ inches long and $1\frac{1}{2}$ inches in diameter and is made of Corning 7740 Pyrex glass that is joined by means of a succession of graded seals to Corning 7052 Kovar sealing glass and then to a 3-inch diameter Kovar sleeve that is welded to the stainless steel flange at the bottom of the pump. Since the sleeve is only $1\frac{1}{4}$ inches long, a strain-relieving section is cut into the flange to accommodate any possible relative variations at the joint and to avoid the propagation of strain to the glass-to-metal seal. The glass partition between the dissociator and the hexapole magnet is ground flat and thinned down to about $\frac{1}{2}$ mm. thickness at the center where the $\frac{3}{4}$ mm. diameter hole is ground through the glass. This hole is located precisely on the axis of the flange, and since the flanges on the pump are also perpendicular and centered to the pump axis, the source aperture of the beam is on the pump axis. Low pressure hydrogen is supplied into the glass tube leading to the discharge through a palladium control valve of new design shown in Figure 4. Source pressure is sensed using a glass bead type thermistor Pirani

Fig. 4. HYDROGEN CONTROL VALVE

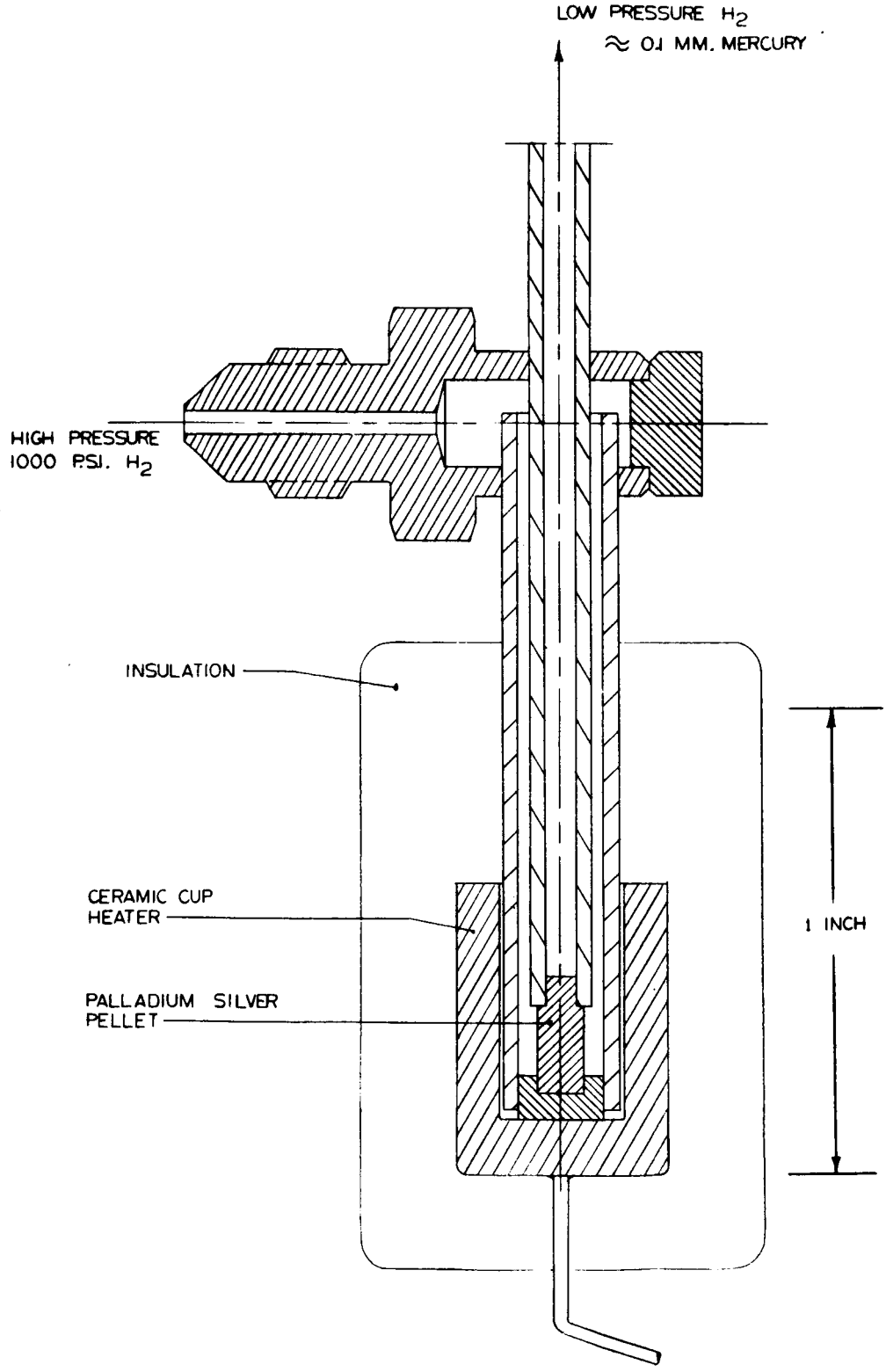

gauge that forms one arm of a bridge circuit. The current across the bridge is servoed to keep the thermistor at a constant temperature, and the self-heating required to do this is a measure of the pressure of the gas that surrounds the thermistor. The current across the bridge is thus a measure of the gas pressure and is used as an input to the pressure servo that operates by heating the palladium pellet until the hydrogen permeation rate through the palladium produces the desired gas pressure at the thermistor.

The atomic hydrogen from the source is directed toward the magnet as a narrow beam using a multitube collimator array of tubes .001" in diameter and .020" long. The array is about 70 per cent transparent to hydrogen and is supplied to us in the form of an array about $\frac{1}{16}$" in diameter mounted in a flat glass plate $\frac{1}{2}$" in diameter that is cemented to the ground surface of the discharge tube. The array is located over the .030" diameter aperture in the source.

A set of r.f. electrodes is placed so as to apply a 100 MHz r.f. electric field across the discharge tube. With 10 watts of power the discharge operates at a bright red color. An investigation of the optical spectrum from 3000Å to 7000Å shows a very strong preponderance of atomic hydrogen spectral lines in the Balmer series and very little background due to molecular hydrogen.

F. THE HEXAPOLE STATE SELECTOR MAGNET

For the satellite maser, the beam trajectory from the source to the bulb is short in comparison to previous maser design. It was decided that the magnet would be designed to focus atoms at the most probable velocity from the source assuming its temperature to be about 400°K. For a hexapole magnet having a $\frac{1}{8}$" diameter bore and a field strength of 8 Kilogauss at the pole tips, the required length is about $3\frac{1}{2}$". A stopping disc is incorporated at the exit of the magnet to prevent undissociated hydrogen and unfocussed high velocity atoms from reaching the bulb. During initial bakeout the disc also reduces possible contamination of the bulb from products baked out from the source.

The design of the magnet is shown in Figure 5. The stopping disc is a glass bead fused onto a platinum wire that is clamped at the end of the magnet. From the figure it is seen that the magnet consists of alternate sections of Alnico 8B and Armco iron.

The magnet is mounted to the upper wall of the pump by means of a yoke about the magnet and held there by three long studs. The magnet angle and lateral position is adjustable by three screws. While this type of mounting is not meant as a prototype for the satellite maser, it is a convenient magnet mounting for testing the operation of the maser.

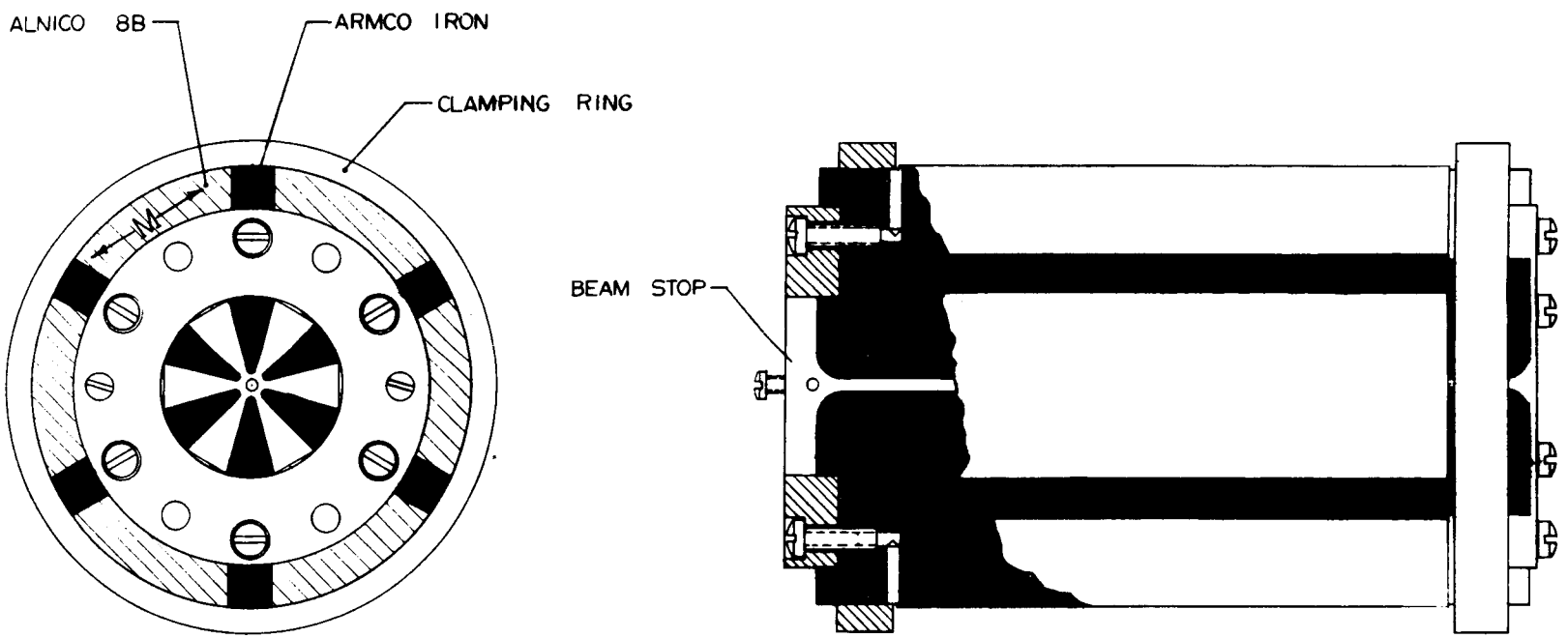

HEXAPOLE FOCUSSING MAGNET

Figure 5.

Fig. 6. Doppler Cancellation Method.

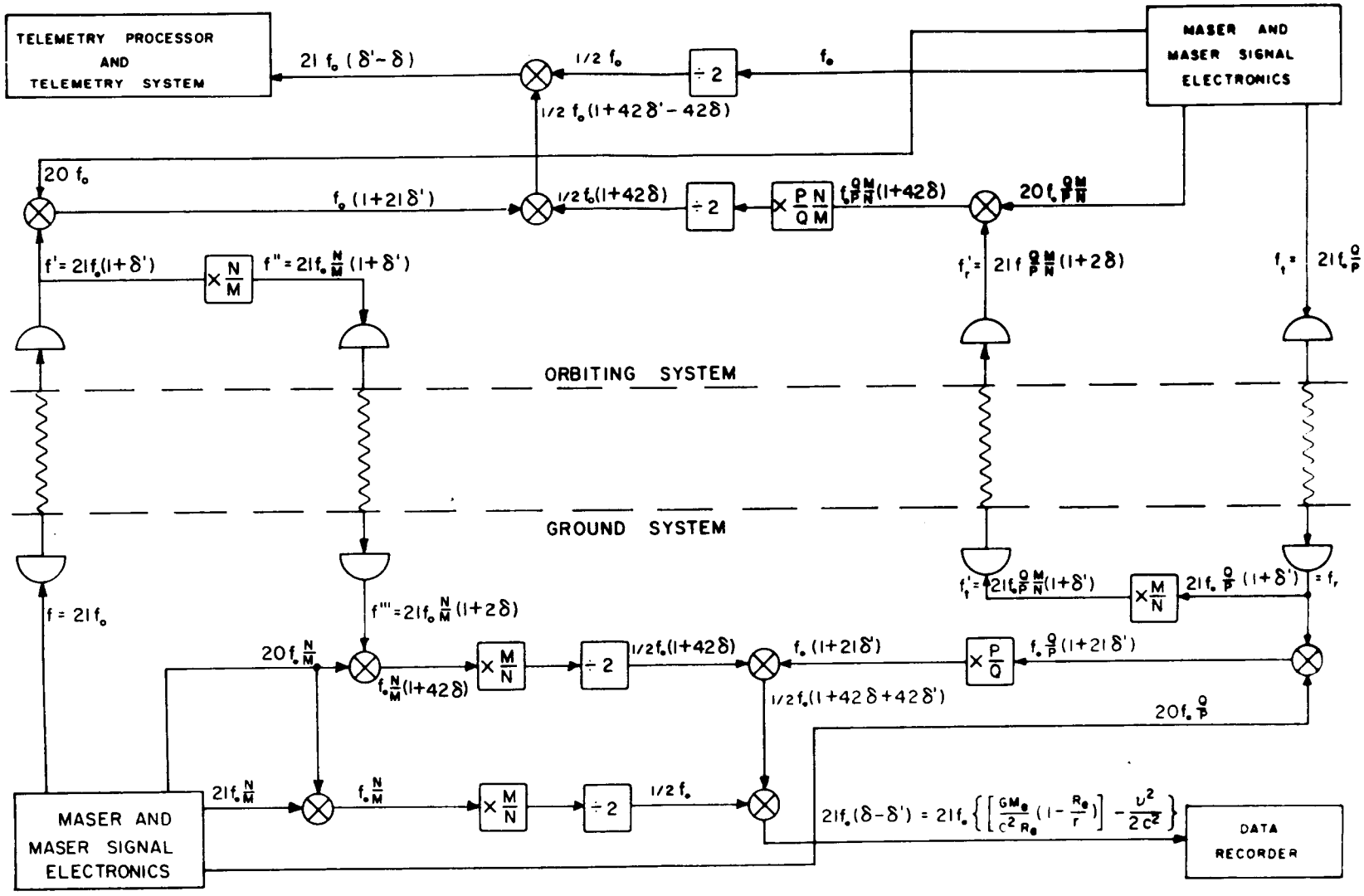

III. TELEMETRY SYSTEM CONSIDERATIONS

A. INTRODUCTION

Some preliminary calculations of the effects that will be important in making the comparison between the ground and space masers have been done and are reported here in two following sections.

The first is a rough calculation of signal-to-noise ratios for the experiment if it is performed using relatively standard equipment for phase-tracking the satellite using a transponder system as shown in Figure 6. The use of this system will remove the possibility of having a systematic error due to the nonreciprocal propagation between the ground and the satellite.

The second section describes the principle of the phase cancellation technique as it applies to the system when one includes second order doppler and gravitation frequency shifts. A block diagram of a system based on the S-band CCS* transponder is given, and typical frequencies in the system are listed.

The purpose of these calculations is to determine some of the requirements for obtaining the data of the gravitational effect on time for this orbit and to relate these requirements to existing equipment and techniques.

B. SIGNAL-TO-NOISE RATIOS

A system for transmitting and receiving the signals to and from the satellite is shown in Figure 6 and has the following properties:

Ground Transmitter		Satellite Transmitter	
Power input	2 kw	Power input	20 watts
Antenna	30' dish	Antenna	½ wave dipole
Gain	43 db	Gain	2 db
Cable losses	3 db		

* The S-IVB Command and Communications System.

Ground Receiver		Satellite Receiver	
Noise figure	10 db	Noise figure	10 db
Predetection bandwidth	100 kHz	Predetection bandwidth	100 kHz
Antenna as above for transmitter		Antenna as above for transmitter	

Signal-to-noise ratios and power levels for a synchronous orbit are described as follows:

Ground to Satellite

+	-	
43 db		Transmitting antenna gain
	3 db	Cable loss
	189 db	Attenuation due to space
2.15 db		Receiving antenna gain, assuming half-wave dipole on the satellite
+45 db	-192 db	
Net	-147 db	

Signal received is -147 db below 2 kw, or -84 dbm.

Noise power at receiver for noise figure 10 db and bandwidth 100 kHz

$= 10\ kTB$

$= 4.2 \times 10^{-15}$ watts

$= -116$ dbm

Signal-to-noise at satellite is 32 db.

Satellite to Ground

Signal received is -147 db below 20 watts, or -104 dbm.

Signal-to-noise at ground is 10 db with no postdetection filtering.

If we average the readings over 24-hour intervals and if the telemetry is at 2 GHz, the required phase determination for a precision of 10^{-14} in $\frac{\Delta f}{f}$ is

$$10^{-14} = \frac{\Delta\phi}{86400} \quad \frac{1}{2\pi \times 2 \times 10^9}$$

$$\Delta\phi = 10.9 \text{ radians}$$

From the magnitudes of the signal-to-noise ratios estimated above and since the orbital doppler frequency shifts are in the order of a few kilohertz.

or less, it is likely that the problem of retrieving the data will be relatively straightforward. In Figure 6, the data is extracted in the form of a low frequency beat signal at about 1.23 Hz. The signal contains both the effects of gravitation and the effects of transverse motion. In order to interpret this data, knowledge of the value of v^2 averaged over the time of observation is required. In view of the 28^0 inclination of the proposed orbit, a knowledge of the position of the satellite is necessary in order to evaluate $\langle v^2 \rangle_{t_{obs}}$. The accuracy required in the determination of v to make a 1×10^{-4} measurement in the total effect in a period of one day is about 2×10^{-4}.

C. RED SHIFT EXPERIMENT TELEMETRY SYSTEM

System S is in motion relative to system O containing the transmitter-receiver system. Ground system proper time units are used.

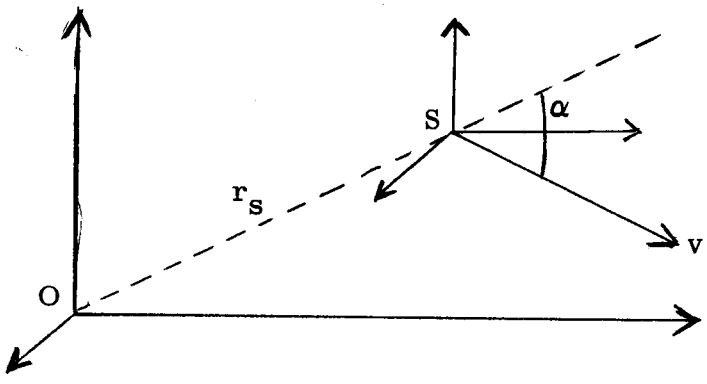

f is frequency transmitted;

$\beta = \frac{v}{c}$;

$\phi = -\frac{GM}{c^2}\left[\frac{1}{r_s} - \frac{1}{R_e}\right]$, where R_e is the earth's radius;

f' is received frequency in terms of proper time of system O.

$$f' = f\,\frac{(1 - \beta\cos\alpha)}{(1 - \beta^2 + 2\phi)^{1/2}}$$

The retransmitted signal at the satellite is obtained by synthesis of the received signal and is given in terms of $\frac{N}{M}f'$, where N and M are integers. In the case of the unified S-band equipment, the values of N and M are 240 and 221, respectively. In one system f is 2101 MHz so that f' is about 2282 MHz.

Let f" be the retransmitted signal. In this case

$$f'' = \frac{N}{M}f' = f\,\frac{N}{M}\,\frac{(1 - \beta\cos\alpha)}{(1 - \beta^2 + 2\phi)^{1/2}}\,.$$

The signal received on the ground is at a frequency f''' where

$$f''' = f\frac{N}{M}\ \frac{(1-\beta\cos\alpha)}{(1-\beta^2+2\phi)^{1/2}}\ \frac{(1-\beta^2+2\phi)^{1/2}}{(1+\beta\cos\alpha)}$$

$$= f\frac{N}{M}\ \frac{(1-\beta\cos\alpha)}{(1+\beta\cos\alpha)}.$$

Expanding this in terms of a power series in β, one gets

$$f''' \approx f\frac{N}{M}\ (1 - 2\beta\cos\alpha + 2\beta^2\cos^2\alpha)$$

where terms in β^3 and higher powers are not included.

The signal can be mixed with a frequency $f\frac{N}{M}$ generated on the ground, and the resulting signal is

$$f_b = f''' - f\frac{N}{M} = f\frac{N}{M}\ (-2\beta\cos\alpha + 2\beta^2\cos^2\alpha).$$

This signal can be fed to a device that will divide the elapsed phase by 2, giving a phase angle

$$\Omega_b t = \frac{2\pi f_b}{2} = f\frac{N}{M}\ (-\beta\cos\alpha + \beta^2\cos^2\alpha)\ 2\pi t$$

The signal from the maser in the satellite can be transmitted at a frequency offset from the "proper frequency" f of the ground based maser clocks by the ratio $\frac{P}{Q}$ so as to avoid interference in the several carriers used. The frequency transmitted will be $f_t = f\frac{P}{Q}$ in the time scale proper to the satellite. When received, the frequency will be

$$f_r = f_t\frac{(1-\beta^2+2\phi)^{1/2}}{(1+\beta\cos\alpha)}$$

$$= f\frac{P}{Q}\ \frac{(1-\beta^2+2\phi)^{1/2}}{(1+\beta\cos\alpha)}, \text{ where P and Q are integers.}$$

Expanding this to second order in β and first order in ϕ,

$$= f\frac{P}{Q}\left[1 - \beta\cos\alpha + \beta^2\cos^2\alpha - \frac{1}{2}\beta^2 + \phi\right].$$

Multiplying this by the ratio $\frac{Q}{P}\ \frac{N}{M}$, one gets

$$f\frac{N}{M}\left[1 - \beta\cos\alpha + \beta^2\cos^2\alpha - \frac{1}{2}\beta^2 + \phi\right].$$

The frequency $\frac{f_b}{2} = \frac{N}{M}\left(-\beta\cos\alpha + \beta^2\cos^2\alpha\right)$ obtained from the transponder link can be subtracted, leaving $f\frac{N}{M}\left[1 - \frac{1}{2}\beta^2 + \phi\right]$ which can be compared with $\frac{N}{M}f$ and so gives the offset due to the gravitational effect and the second order doppler effect, Δf_{GD}.

$$\Delta f_{GD} = f\frac{N}{M}\left[1 - \frac{\beta^2}{2} + \phi\right] - f\frac{N}{M}$$

$$\Delta f_{GD} = f\frac{N}{M}\left[\phi - \frac{\beta^2}{2}\right].$$

The fractional effect is

$$\frac{\Delta f}{\frac{N}{M}f} = \phi - \frac{\beta^2}{2}.$$

The first term, ϕ, is given by

$$\phi = \frac{GM}{R_e c^2}\left[1 - \frac{R_e}{r}\right]$$

where G is gravitational constant
M is mass of earth
R_e is radius of earth
c is velocity of light
r is radius of spacecraft orbit
m is mass of satellite.

From the mechanics of a simple circular orbit,

$$\frac{mv^2}{r} = \frac{GmM}{r^2}$$

$$\frac{1}{2}\frac{v^2}{c^2} = \frac{1}{2}\frac{GM}{rc^2} = \frac{\beta^2}{2}$$

so that the total effect $\phi - \frac{\beta^2}{2}$ is given by

$$\phi - \frac{\beta^2}{2} = \frac{GM}{R_e c^2}\left[1 - \frac{3}{2}\frac{R_e}{r}\right].$$

The effects of propagation variations due to the dielectric of the atmosphere will, to a large extent, be averaged to zero by this technique if the periods of the variations are long compared to the 0.2 second round-trip time of a wavefront from the transmitter. Normal atmospheric variations occur more slowly than this. Since the system will measure accumulated phase due to the coherence of the outbound and inbound signals, the phase information will allow averaging of frequency such that the r.m.s. deviation of the measured frequency shifts will be reduced proportionally to $1/t_{obs}$. By making the observation time, t_{obs}, long compared to 0.2 sec., the accuracy of measurement of frequency can be improved such that the telemetry is not the limiting factor in the clock comparison.

One must be aware of effects due to systematic dielectric motion and nonreciprocal propagation through the ionosphere. In particular, a consistent upward thermal air flow, common in the tropics, might offer a systematic frequency shift in the result. This is possible since the averaging of the propagation velocity over a two-way path is not the same as the propagation velocity over the one-way path from the satellite to the earth.

Such effects, if they are significant, can be measured and accounted for by a second transponder system on the ground that would return to the satellite the signal originally transmitted at proper time frequency $f_t = f\frac{P}{Q}$ offset by a ratio $\frac{S}{T}$. The received ground signal at proper time frequency f' would then be compared in the satellite in the same way as discussed for the ground system, and the phase difference recorded. A comparison of the records would then allow the measurement of such systematic effects. The resulting data would thus "close the loop" on any systematic propagation effects.

The choice of transmitter frequencies and offset ratios should be such as to keep the frequencies high and reasonably close together to remove the possibility of having variation of propagation velocity with frequency. Since the bandwidths of the signals are small, the signals can all be in narrow bands of allocated frequencies.

IV. ELECTRONICS

A. AUTOMATIC TUNING SYSTEM

1. Theory of Operation

The oscillation frequency of a hydrogen maser is "pulled" by the maser cavity resonator. The degree of pulling depends on the cavity detuning and the atomic resonance linewidth in the following way:*

$$\nu = \nu_H + \left[\frac{\nu_c - \nu_H}{\nu_c} \quad Q - \frac{0.29\,\bar{v}\,a_0^2\,\hbar\,V_c}{Q\mu_0^2\,\eta\,V_b}\right]\Delta\nu_\ell \tag{1}$$

where
- ν = Maser oscillation frequency
- ν_H = Atomic resonance frequency
- ν_c = Cavity center frequency
- Q = Quality factor of cavity
- $\bar{v}$ = Mean velocity of the hydrogen atom
- a_0 = First Bohr orbit radius
- $\hbar$ = Planck's constant divided by 2π
- μ_0 = Bohr magneton
- V_c = Volume of cavity
- V_b = Volume of storage bulb
- η = Ratio of average electromagnetic field energy density in the bulb to average energy density taken over the cavity
- $\Delta\nu_\ell$ = Atomic resonance linewidth

It is apparent that if the cavity is tuned to

$$\nu_{c_0} = \nu_H\left[\frac{1}{1 - \frac{0.29\,\bar{v}\,a_0^2\,\hbar\,V_c}{Q^2\mu_0^2\,\eta\,V_b}}\right] \tag{2}$$

then the term in the brackets in equation (1) vanishes and

$$\nu = \nu_H \tag{3}$$

that is, the maser oscillates at exactly the center of the atomic resonance line.

* J. Vanier and R.F.C. Vessot, Appl. Phys. L. 4, 122 (1 April 1964).

Fig. B-1. Automatic Tuning System.

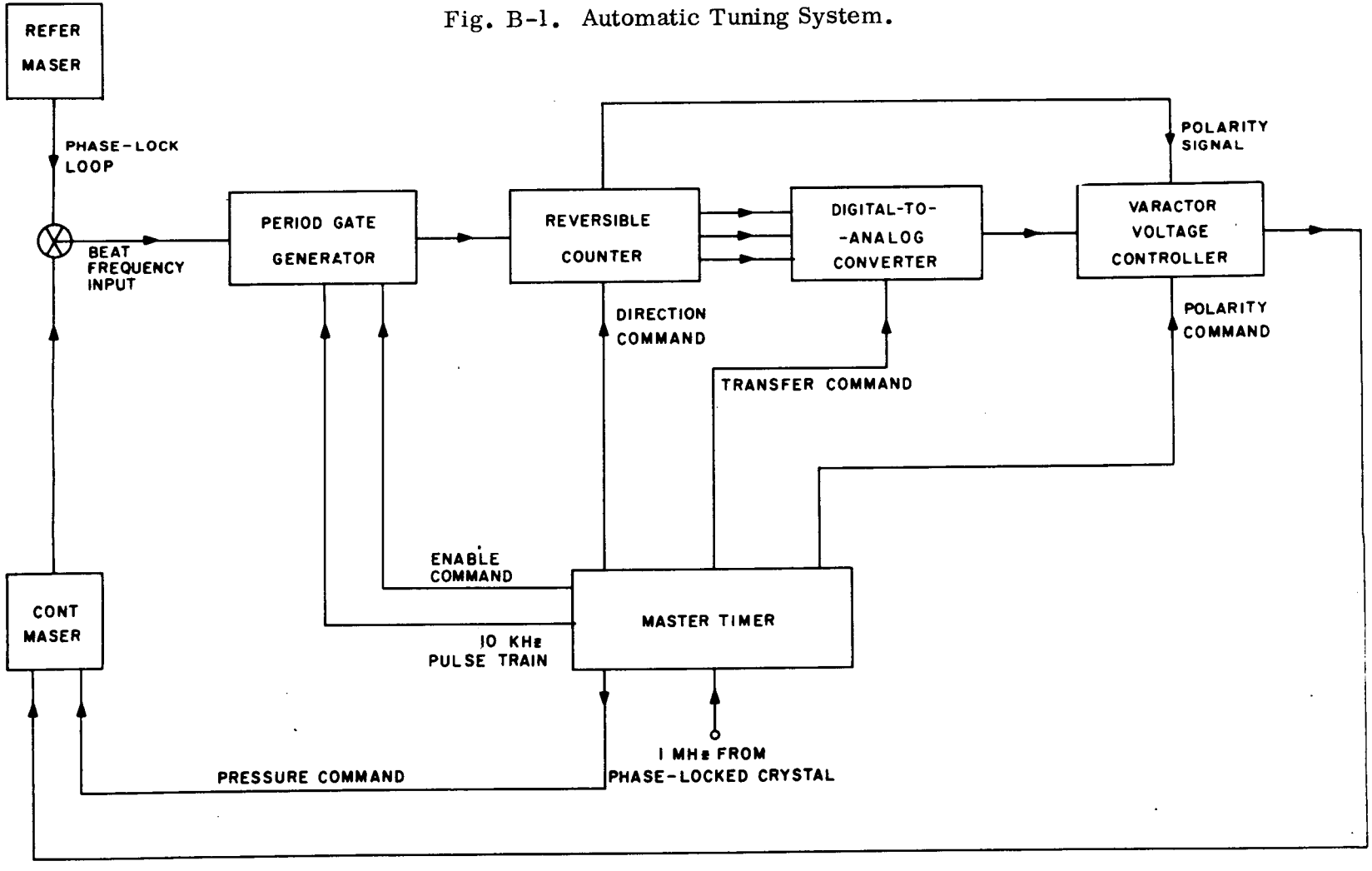

The cavity can be tuned to ν_c by making use of the fact that the linewidth $\Delta\nu$ is proportional to I_{tot}, the total flux of atoms entering the bulb. It can be shown that

$$\Delta\nu_{S.E.} = \frac{1}{\pi\sqrt{2}} \frac{T_b}{V_b} \sigma \bar{v} I_{tot} \tag{4}$$

where $\Delta\nu_{S.E.}$ is the spin exchange contribution to the linewidth and T_b is the mean storage time of the bulb. It can be seen from equation (1) that at the correct cavity tuning point, ν_{c_0}, ν is independent of I_{tot}, the total hydrogen flux. The criterion for correct cavity tuning is that no shift in maser oscillation frequency results from a change in the flux of atomic hydrogen.

2. Detailed System Analysis

The automatic tuner exploits the physical phenomena described in the previous section. The system is capable of retuning two initially detuned masers and of holding this tuned condition indefinitely. A feasibility model of the automatic tuner was constructed using decimal arithmetic and commercially available components wherever possible. The system analysis and circuit description below is based on this feasibility model, as are the test results. The binary computer, a breadboard of the in-flight computer, is described in a later section.

Operation of the Automatic Tuner-- The automatic tuner operates on the beat between the controlled maser and a reference maser. The reference maser is offset in frequency by means of a synthesizer in the phase lock loop. This offset, in the order of 4×10^{-11}, eliminates the necessity for determining if the controlled maser is higher or lower in frequency than the reference and also avoids the possiblity of excessively long beats.

The low frequency beat is fed into the input of the period gate generator as shown in the block diagram, Figure B-1. The period gate generator produces a gating signal which begins at the first positive-going zero crossing of the beat input after an enabling pulse from the master timer and which ends after 1, 10, 100 or 1000 periods of the input as selected by a switch. This

Fig. B-2 Tuning Cycle.

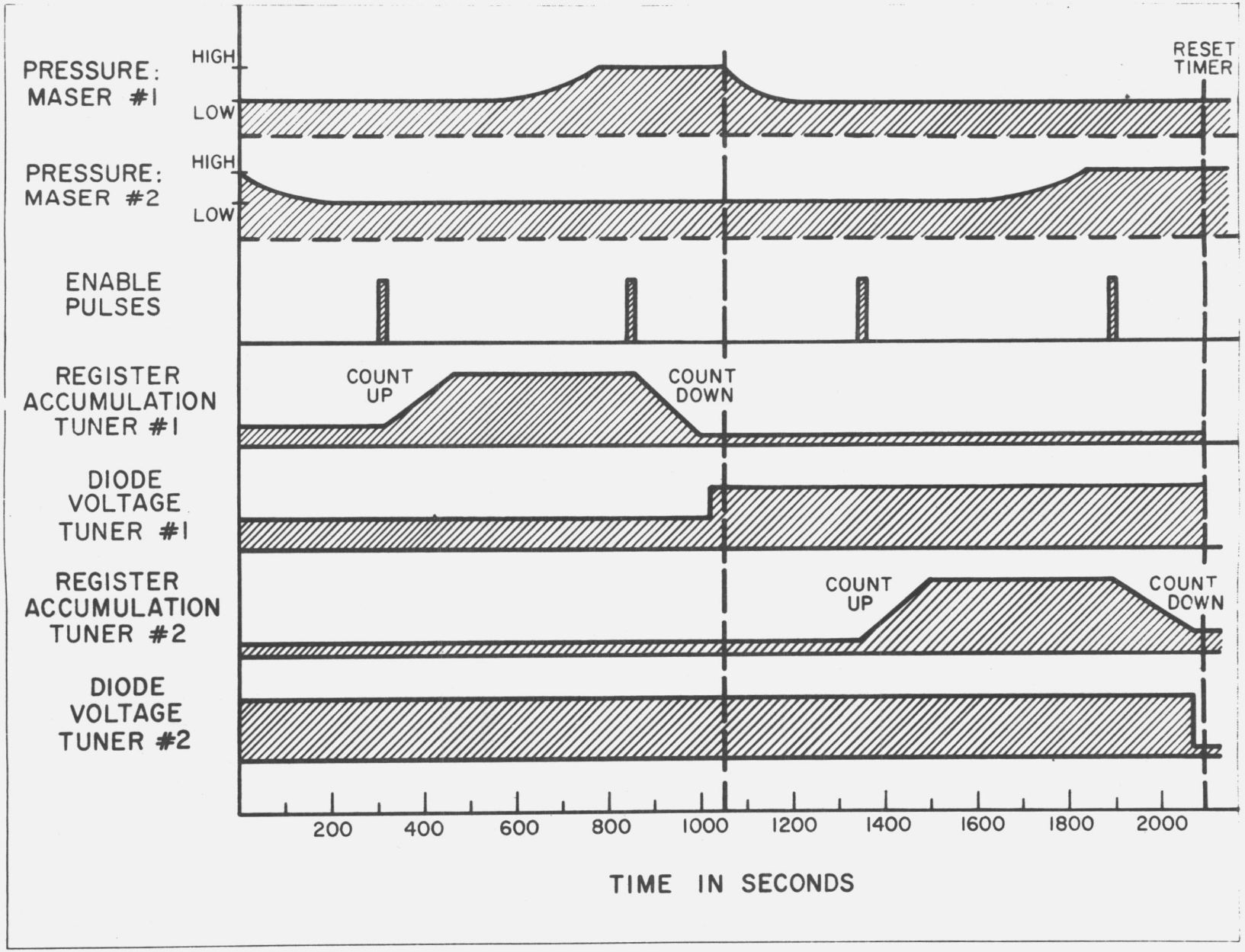

gating pulse closes the master gate, also located in the period gate generator, allowing the reversible counter to accumulate a 10kHz pulse stream supplied from the master timer.

The digital-to-analog converter produces, on command, an analog voltage proportional to the digital reading in the register of the reversible counter. This analog voltage is amplified and processed in the varactor voltage controller and then used to control the varactor tuner in the maser cavity.

The pressure control provides for the presetting of two hydrogen pressure levels in the maser and for switching between these two pressures under control of the master timer.

Figure B-2 is a sequence drawing, illustrating the operation of the automatic tuning cycle for two masers in proper time sequence. The elapsed times shown are typical for the tests run on the feasibility model of the automatic tuner. The time sequence of the tuning cycle is as follows:

a) An initial command from the master timer at time $t = 0$ sets the pressure of the controlled maser to a low level and also sets the reversible counter to read "up."

b) At $t = 300$ seconds, allowing the controlled maser pressure time to stabilize, the master timer enables the period gate generator, starting the period measuring process. The reversible counter measures the period (or a multiple of the period) of the beat, counting up on the 10 kHz pulse stream from the master gate.

c) At $t = 550$ seconds, a command from the master timer sets the pressure of the controlled maser to a relatively high flux level and sets the counter to count down.

d) At $t = 850$ seconds, the period gate generator is again "enabled" and the counter again digitally measures the beat period (or a multiple thereof), this time counting downwards. The number remaining in the counter register is a measure of the change in frequency of the controlled maser resulting from the change in hydrogen flux. As can be seen from Figure B-3, if the reference maser is offset to a frequency higher than the controlled

$$\text{COUNTER RESIDUE} = \left[\frac{1}{\nu_{M2}} - \frac{1}{\nu_{MI\,(LOW\ PRESS.)}}\right] - \left[\frac{1}{\nu_{M2}} - \frac{1}{\nu_{MI\,(HIGH\ PRESS.)}}\right]$$

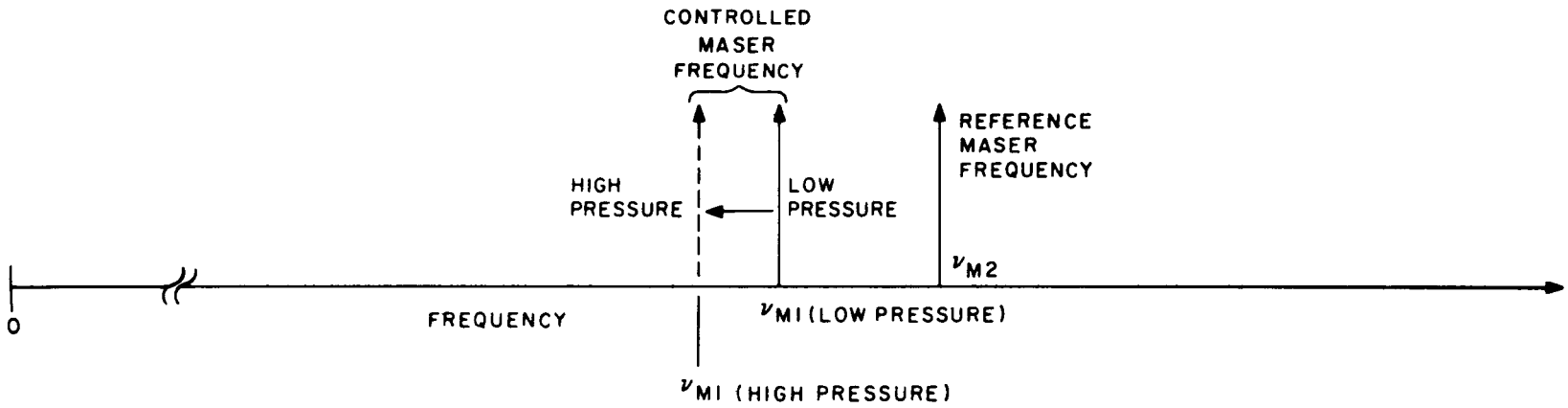

Fig. B-3. Maser Frequency Offset and the Deviation of the Sign of the Counter Residue.

maser, the residue in the register will be positive if the controlled maser frequency goes down with increasing flux (and negative if the maser frequency goes up with increasing flux). An electrical signal indicating the sign of residue in the register is fed to the varactor voltage controller.

e) At t = 1040 seconds a command from the master timer transfers the binary-coded digital residue in the counter register to the register in the D-A converter. The converter produces an analog voltage proportional to the digital residue which is amplified and processed in the varactor voltage controller. The magnitude and sign of the gain of the varactor voltage controller is adjusted for negative feedback; in the situation illustrated in Figure B-3, the change in voltage should be such as to raise the frequency of the maser cavity frequency as shown by the dotted lines.

Note that the magnitude of the analog voltage is proportional to the numerical value of the residue in the counter; the sign of the correction depends on the sign signal from the counter register.

f) At t = 1050 seconds, the master timer is reset to zero. However, the "cycle" control is toggled, interchanging the roles of the reference and controlled masers. The cycle now repeats, tuning the second maser. At the next reset, the cycle control is again toggled, and the first maser is again tuned. Manual overrides are provided to modify the sequence if desirable.

The varactor voltage is automatically readjusted on each cycle until there is no further change in the counter residue. It should be noted that this system is a true integrating digital servo; there is no possibility of a steady-state error except for the granularity of the digital-to-analog conversion.

3. Detailed Circuit Analysis -- Feasibility Model

Period Gate Generator -- Figure B-4 is a circuit diagram of the period gate generator. The beat input is fed to Q1, an integrated circuit operation amplifier. The amplifier stage is d. c. coupled and carefully designed to minimize drift and high frequency noise. Q2 is also an integrated operational amplifier, arranged as a Schmitt trigger.

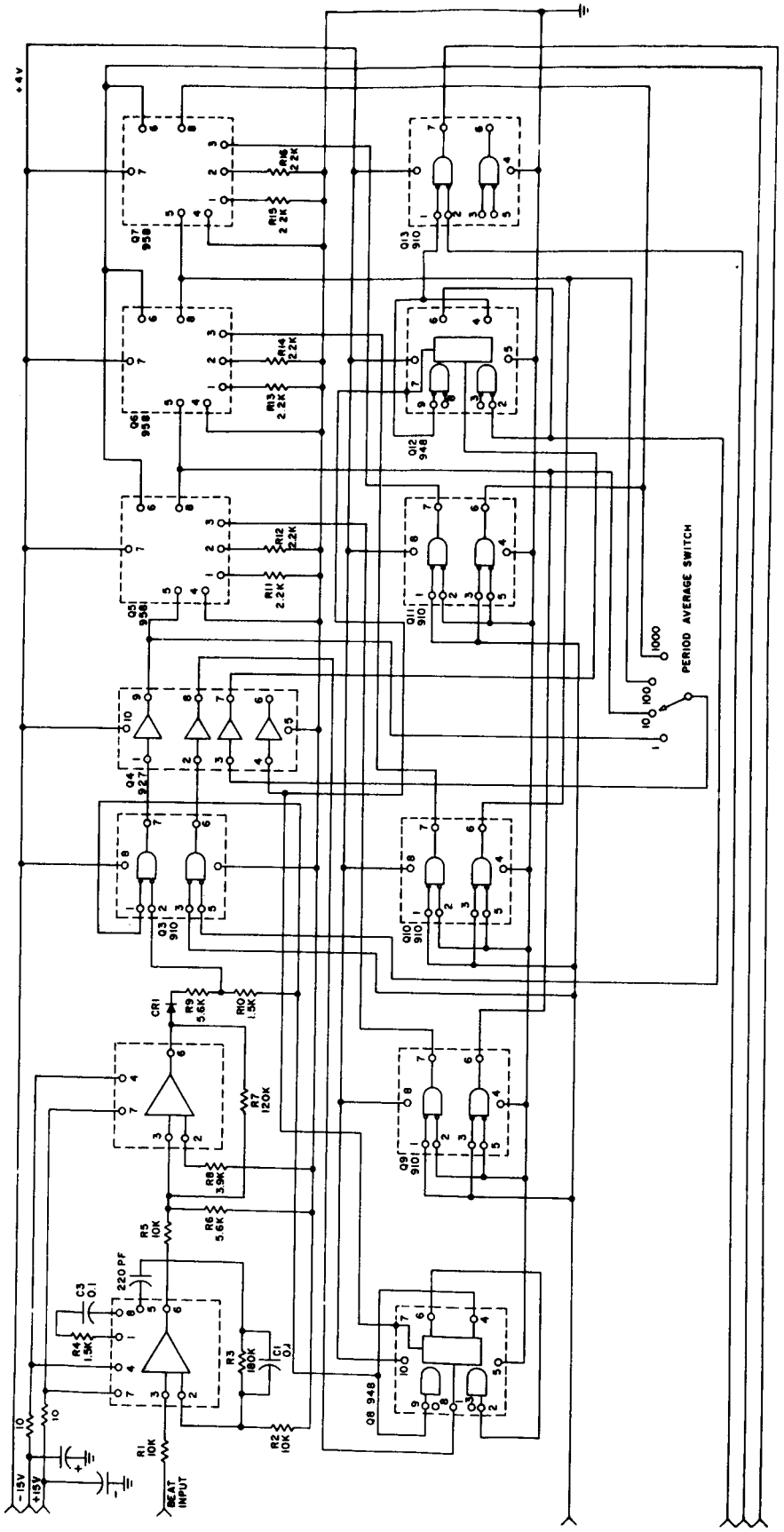

Fig. B-4. Period Gate Generator.

The square-wave output from the Schmitt trigger state is one input to the number 1 nand gate of the integrated dual two-input nand gate, Q3. The gate is normally held open by a logic signal from the output of the integrated J-K flip-flop, Q8. The negative-going transition of the enable pulse triggers Q8, which in turn closes gate 1 of Q3. In the one position of the period average switch, the square-wave output of Q2 is transmitted directly to the integrated J-K flip-flop, Q12. Since the J-K flip-flop changes state only on negative transitions, the output of Q12 is a pulse, the length of which is equal to one period of the input beat signal. This period pulse serves two functions: it opens gate 1 of the dual nand gate Q13 to permit the pulse stream from the "pulse input" jack to appear at the "gated pulse out" jack; the trailing edge of the gating pulse retriggers the J-K flip-flop Q8 through gate 2 of Q3, thus opening gate 1 of Q3 and terminating the period measuring process until another enable pulse is received.

In the 10, 100 and 1000 positions of the period average switch, integrated decade counters Q5, Q6 and Q7 are successively switched into the circuit. Since each decade counter produces an output pulse only after ten input pulses, the length of the gating signal applied to gate 1 of Q13 is equal in length to 1, 10, 100 or 1000 periods of the beat input, as selected by the period average switch.

Bidirectional Counter-- The output of the period gate generator is a stream of pulses, at a 10 kHz rate, for an interval of 1, 10, 100 or 1000 periods of the beat between the two masers. The accumulated count on the bidirectional counter register is equal to the time duration of 1, 10, 100 or 1000 periods, respectively, measured in tenths of milliseconds.

The bidirectional counters are standard commercial units, Hewlett-Packard Type 5280A. The directional information to the counter is in the form of a d.c. logic level to channel B of the counter as shown in Figure B-1; the command pulses from the master timer are converted to d.c. logic levels by integrated circuit bistable flip-flops in the count and polarity control unit; the circuitry is quite straightforward and need not be detailed here.

Digital-to-Analog Converter-- The digital-to-analog converters have a low d.c. drift rate and were especially designed for this application. Any four digits in the counter register can be transferred to the D-A register by the transfer command from the master timer. The digit transference is a "jam" transfer; the D-A register is not reset before the transfer command.

The analog voltage output from the D-A converter is always proportional to the count in the register. A transfer command is generated only once per timing cycle, after a full up and down count, so that the output of the D-A changes only once per cycle.

Varactor Voltage Controller-- The output of the D-A converter goes to the summing terminal of the integrated circuit operational amplifier, Q1, in Figure B-5. The gain of this stage, and therefore the loop gain of the servo, is adjustable by means of the variable feedback resistor R1.

The varactor diode is normally reverse-biased at the output of driver stage. Q2 must therefore always be positive with respect to ground. The "manual" control permits setting the quiescent output level of Q2 at any level between +1 and +14 volts. In order to obtain fully reversible feedback it must be possible to increase or decrease the varactor voltage about the quiescent level set by the "manual" control. The polarity control is accomplished by means of the FET analog gates Q3 and Q4. When Q3 and Q4 are closed, the feedback voltage is applied to the inverting terminal of Q3 and the correction voltage is added to the quiescent output of Q2. If Q3 and Q4 are open, the feedback voltage is applied to the noninverting terminal and subtracts from the quiescent voltage. The FET gates are ideally suited for this application as they have extremely low "on" resistances, in the order of 25 ohms, low leakage current, and zero offset voltage. Furthermore, the series-shunt gate is designed to minimize input current offset of Q2.

The polarity information is carried by the sign of the count in the bidirectional counter register. The sign output from the counter is used to steer the analog gates at the input to Q2 so as to increase or decrease the varactor voltage. Since the counter register is also used for counting up and down, the sign output cannot be used directly to control the analog gates

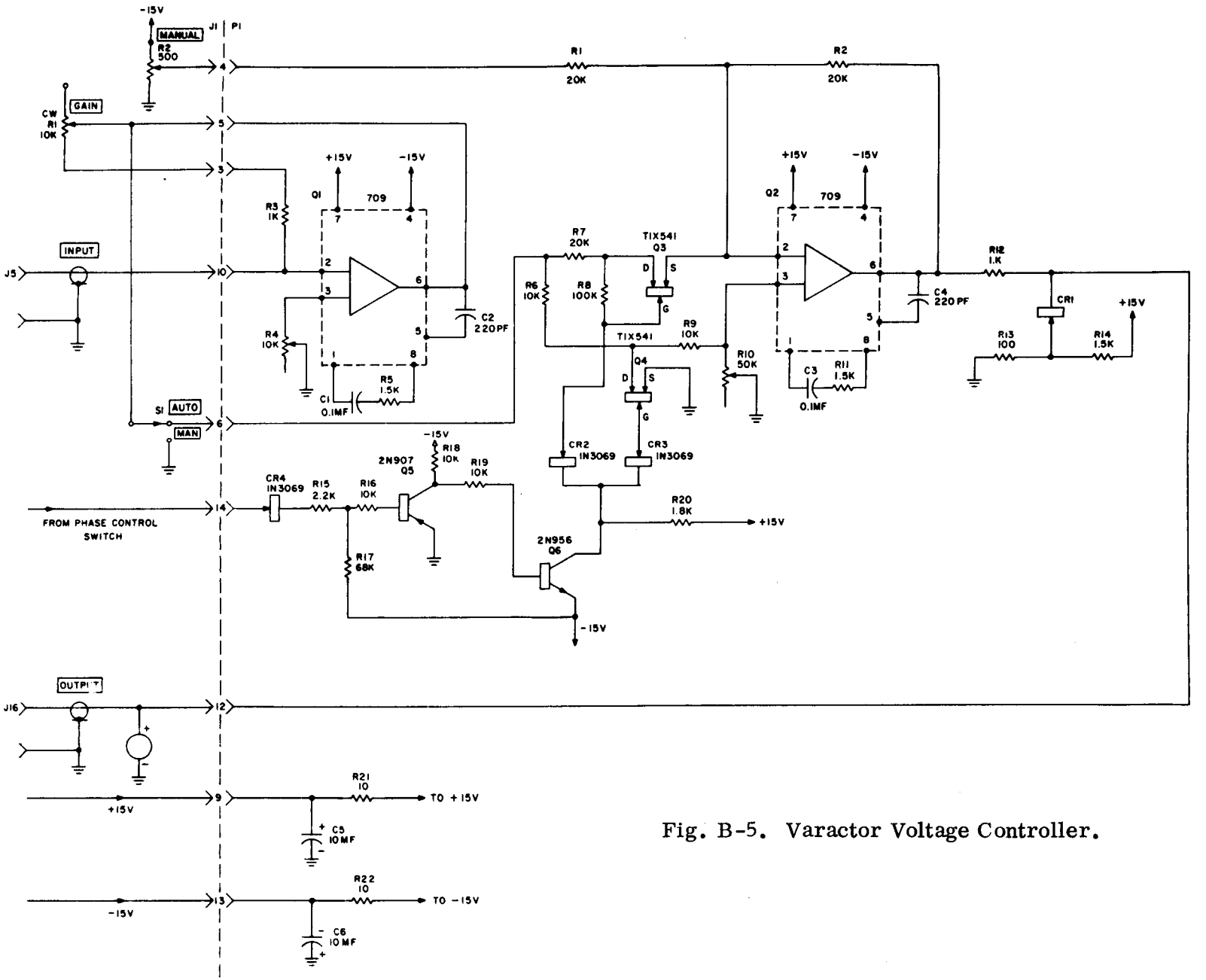

Fig. B-5. Varactor Voltage Controller.

but must be stored in a sign register, which is an integrated circuit J-K flip-flop physically located in the count and polarity control unit. After the bidirectional counter completes its up and down counting cycle, a polarity command from the master timer transfers the sign command from the sign register to the analog gates.

Pressure Control -- The pressure control assembly is shown schematically in Figure B-6. In the H-10 masers, the hydrogen pressure is set by applying a d.c. voltage to the Pirani gauge servo system. The pressure control assembly permits the presetting of two pressure levels by means of the ten-turn potentiometers labeled "Pressure 1" and "Pressure 2" and the remote selection of either pressure setting by means of the FET gates Q8 and Q9.

The integrated circuit bistable flip-flop, Q3, is triggered by the pressure control commands from the master timer. In state 1, Q3 turns off Q4 which turns off Q5. The gate of Q9 rises to the source voltage and Q9 is turned "on," connecting the wiper of the "Pressure 1" potentiometer to the maser. In the second channel Q6 and Q7 are turned on which clamps the gate of Q8 at -15 volts and turns off gate Q8. In pressure state 2, the situation is reversed; Q8 is on and gate Q9 is off.

4. Construction -- Feasibility Model

The complete automatic tuner can be seen in the photograph, Figure B-7. The upper panel is the master timer patch panel. The next two panels house the circuit cards for the period gate generator, varactor voltage controls, pressure controls and digital-to-analog converters. Operating controls and status lights are mounted on the panels. The two bidirectional counters are mounted directly below the circuit card racks.

5. Results -- Feasibility Model

Stability measurements and tuning runs have been made with the system shown in Figure B-8. Two identical double-conversion receivers are used. The uppermost receiver in Figure B-7 phase locks a 5.0 MHz crystal

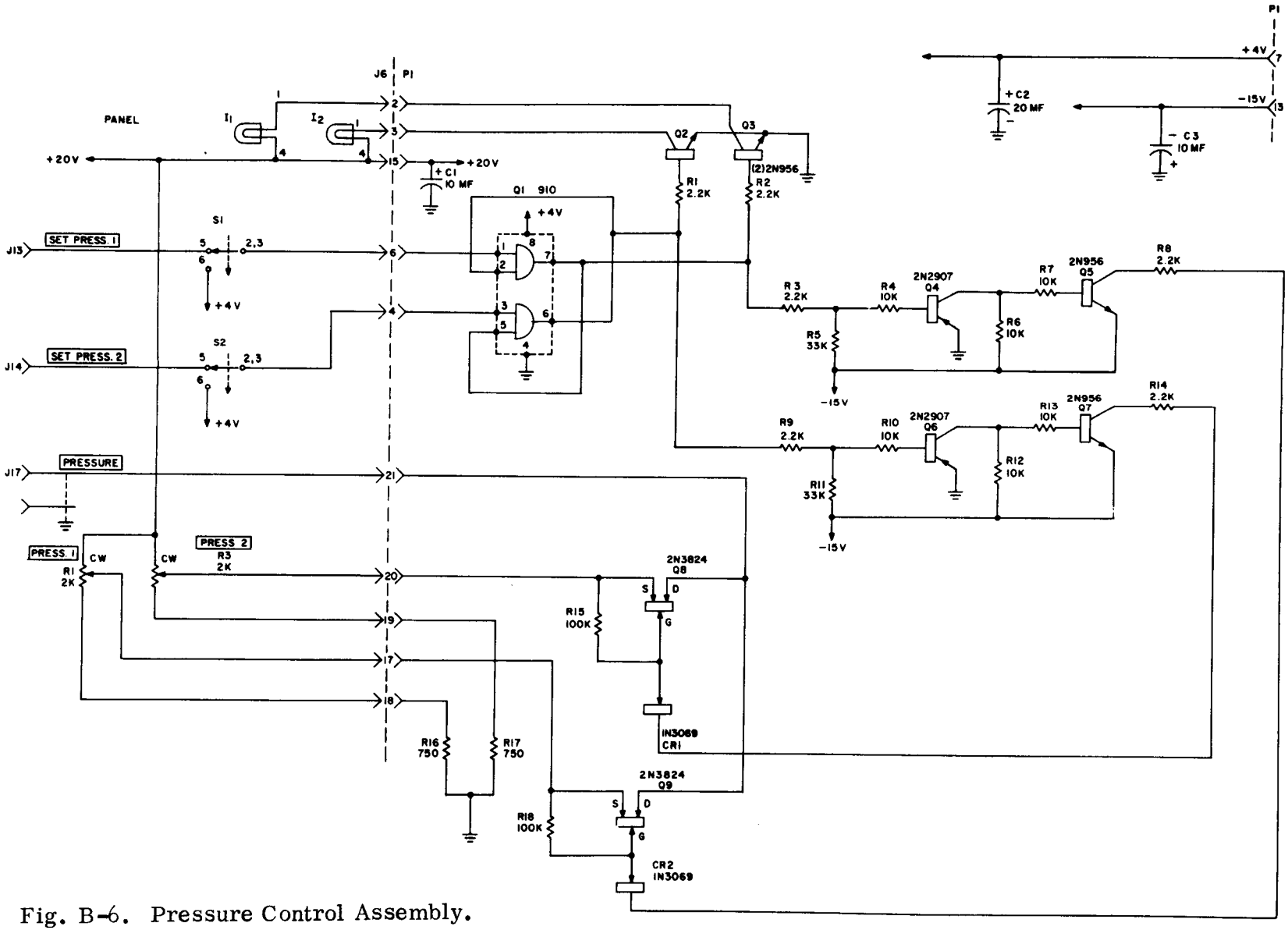

Fig. B-6. Pressure Control Assembly.

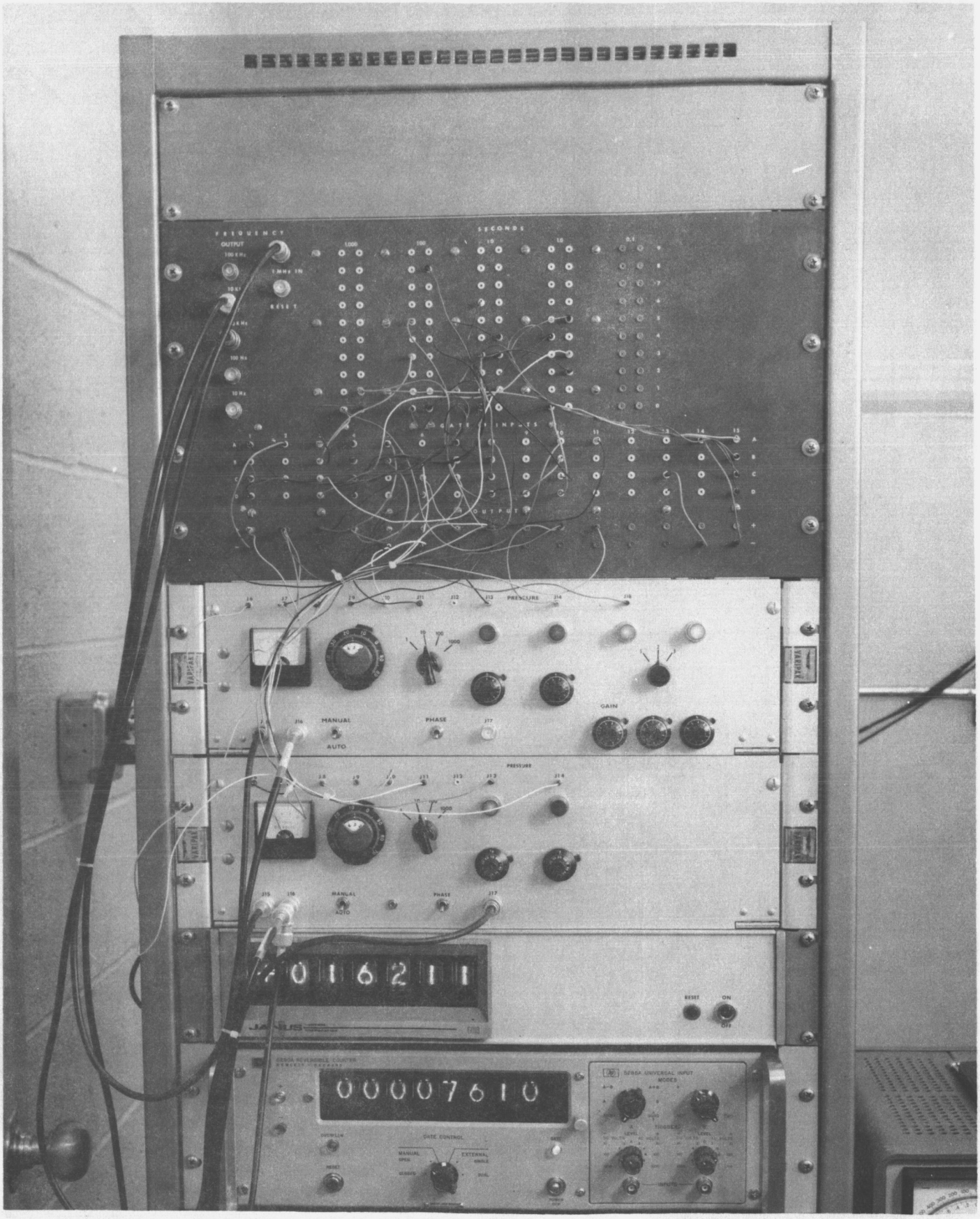

Fig. B-7. Self-Tuning Computer.

oscillator to the output of the first maser; the output of the second receiver is a sinusoidal signal at a frequency

$$\nu_0 = \nu_D + \nu_S \tag{5}$$

where ν_D = Frequency difference between the controlled and reference masers

ν_S = Frequency difference between the two synthesizers

Normally, $|\nu_S| >> |\nu_D|$ so that there is no possibility of ambiguity or excessively long beats. All of the measurements described in this section were taken with $\nu_S = 0.6$ Hz.

A typical tuning run is illustrated in Figure B-9. The tuning varactor voltage for Maser No. 1 was recorded on the upper track and the varactor voltage for Maser No. 2 on the lower track. Full scale for both tracks is 2.0 volts and one major division in the time axis is ten minutes. On the center track is an analog record of a digital measurement of the beat between the two masers with a full-scale range of 2.5×10^{-11}. The synthesizers in the phase lock loops were offset by 0.6 Hz and 100 period averages were taken so that the observation time for each measurement was 166 seconds.

Maser No. 1 was deliberately detuned by arbitrarily setting the tuning diode voltage to 5.0 volts. The corresponding initial frequency error was about 3.8×10^{-12}. Similarly, Maser No. 2 was offset about 5.5×10^{-12} by setting its diode voltage to an arbitrary 4.0 volts.

The loop gain on each tuner was deliberately reduced to effectively demonstrate the tuning operation. The correction process proceeded smoothly, as can be seen from the recording, alternating from Maser No. 1 to Maser No. 2. After 150 minutes the initial total error of 8×10^{-12} was reduced to less than 5×10^{-13}. Of particular interest are the fluctuations in the beat period due to the pressure changes which can be seen clearly for the first 60 minutes of the recording. These fluctuations damped out rapidly, as would be expected, as proper tuning was approached.

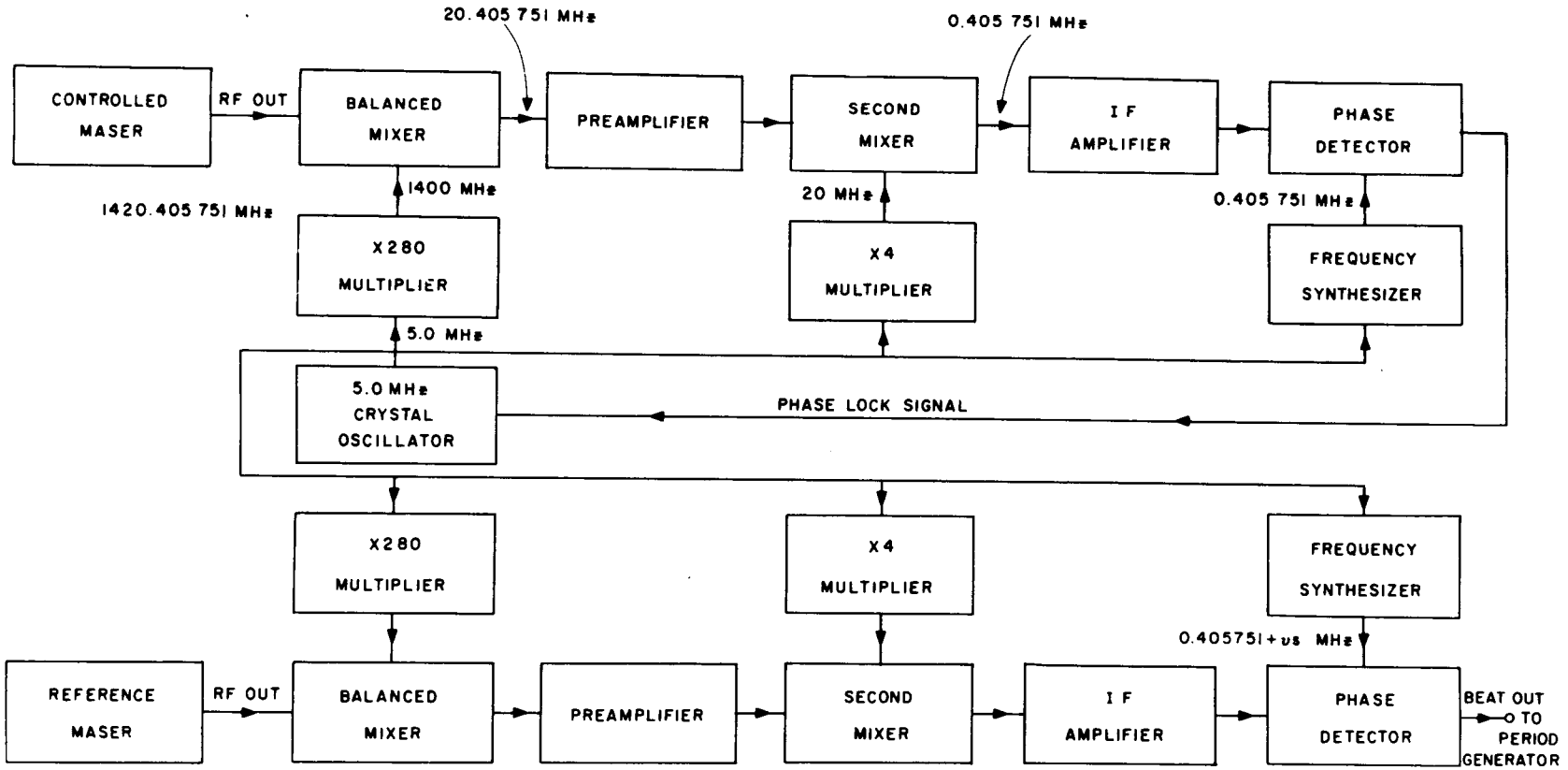

Fig. B-8. Phase-Lock Receiver for Maser Comparison.

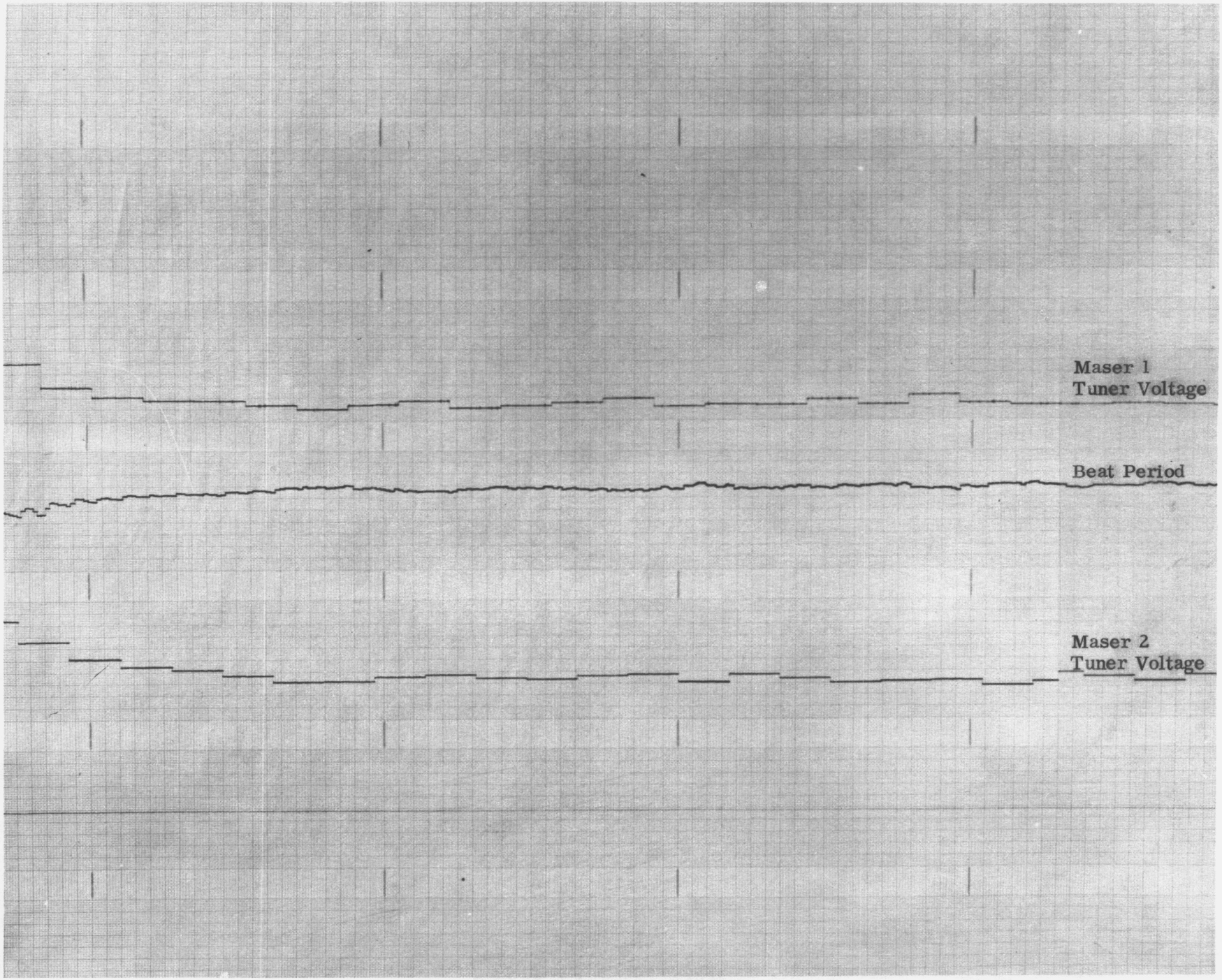

Fig. B-9. Data from Self-Tuner.

Fig. B-10. Stability Data.

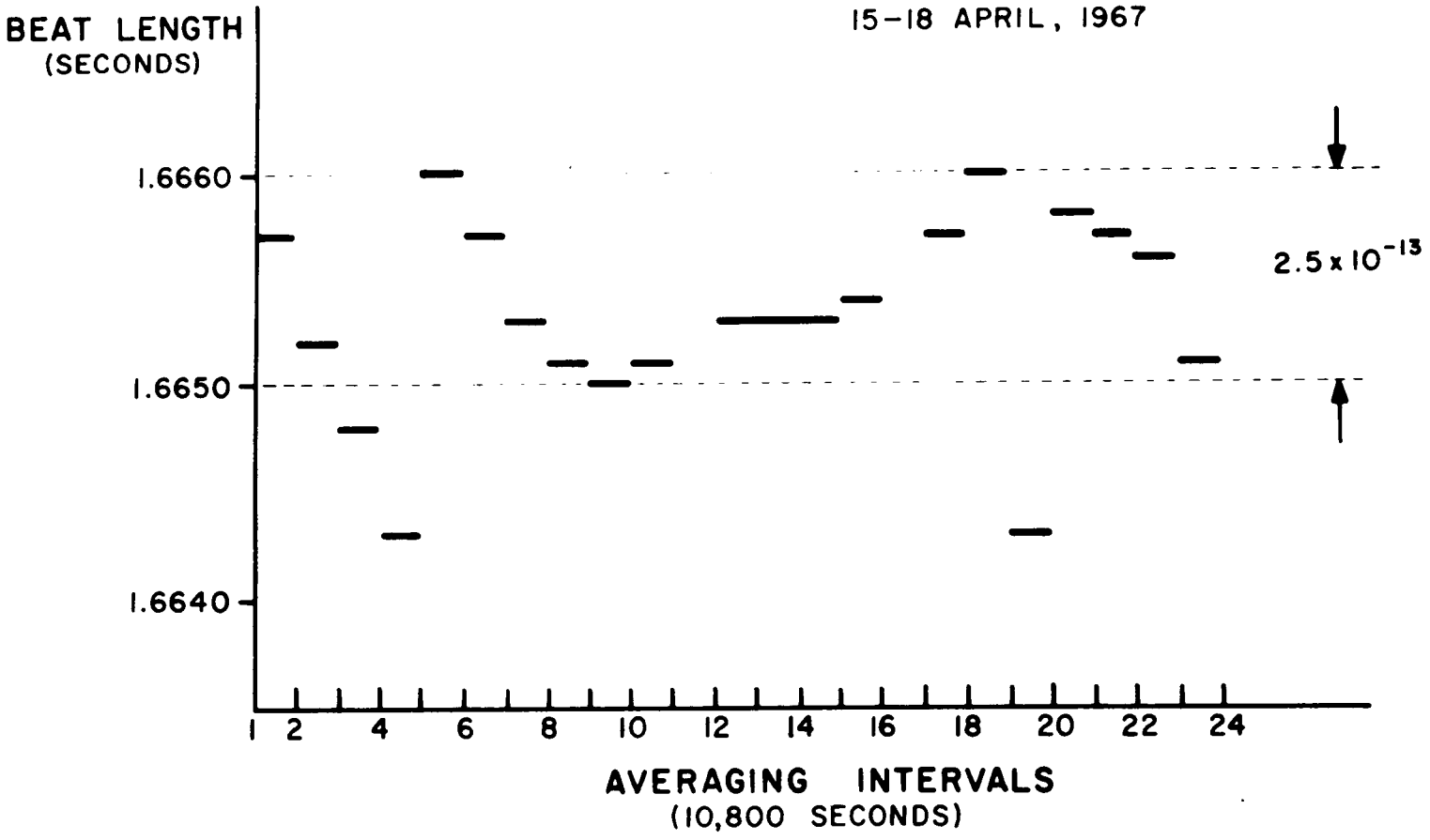

MEAN = 1.6653 SEC.
RMS = 4.67×10^{-4} SEC. (1.18×10^{-13})

Results for a typical three-day run are shown in Figure B-10. The synthesizer offset was 0.6 Hz and the counting interval for each measurement was 166 seconds. Sixty counts were averaged for each data point shown in the figure. All three-hour averages were within $\pm 2.5 \times 10^{-13}$ of the mean with an r.m.s. of approximately 1.2×10^{-13}. Later data, taken through 5 May 1967, shows similar behavior with no detectable drift of the long term mean.

6. Circuit Analysis of Binary Autotuner Computer

A breadboard model of the space-borne automatic tuning computer has been constructed and bench tested. The unit is built entirely of integrated circuits selected from the GSFC Preferred Parts List, except for the twelve-bit digital-to-analog converter. Improvements in circuit design have permitted significant simplifications of the reversible counter and varactor voltage controller. Specifically, the zero sensing and automatic count direction circuitry has been eliminated from the counter and the polarity-sensing and automatic polarity-switching circuits have been eliminated from the varactor voltage controller.

Period Gate Generator--Figure B-11 is a circuit diagram of the period gate generator. The low frequency beat between the controlled maser and the reference maser is d.c. coupled to Z1 on Card A, which is a stable, integrated-circuit, operational amplifier with an upper cut-off frequency of about 3.0 Hz. Z2 is a second operational amplifier, functioning as a low-jitter Schmitt trigger. An upper limit of ± 0.01 percent for the inherent triggering error of this Schmitt trigger has been established.

The square-wave output of the Schmitt trigger is buffered by amplifier Z3 and coupled to the master gate, Z1, on Card B. This gate is held open by the integrated J-K flip-flop, Z8. The enabling pulse, which initiates the period measuring process, triggers Z8, which in turn closes gate Z1. The square-wave output from Card A then triggers flip-flop Z2; the output of Z2 is a pulse of length equal to one period of the input beat signals. The output of Z2 triggers Z3, the output of which is equal to two periods of the input signal, and so on to Z6, which produces a pulse 16 periods in length.

Fig. B-11. Circuit Diagram of Period Gate Generator.

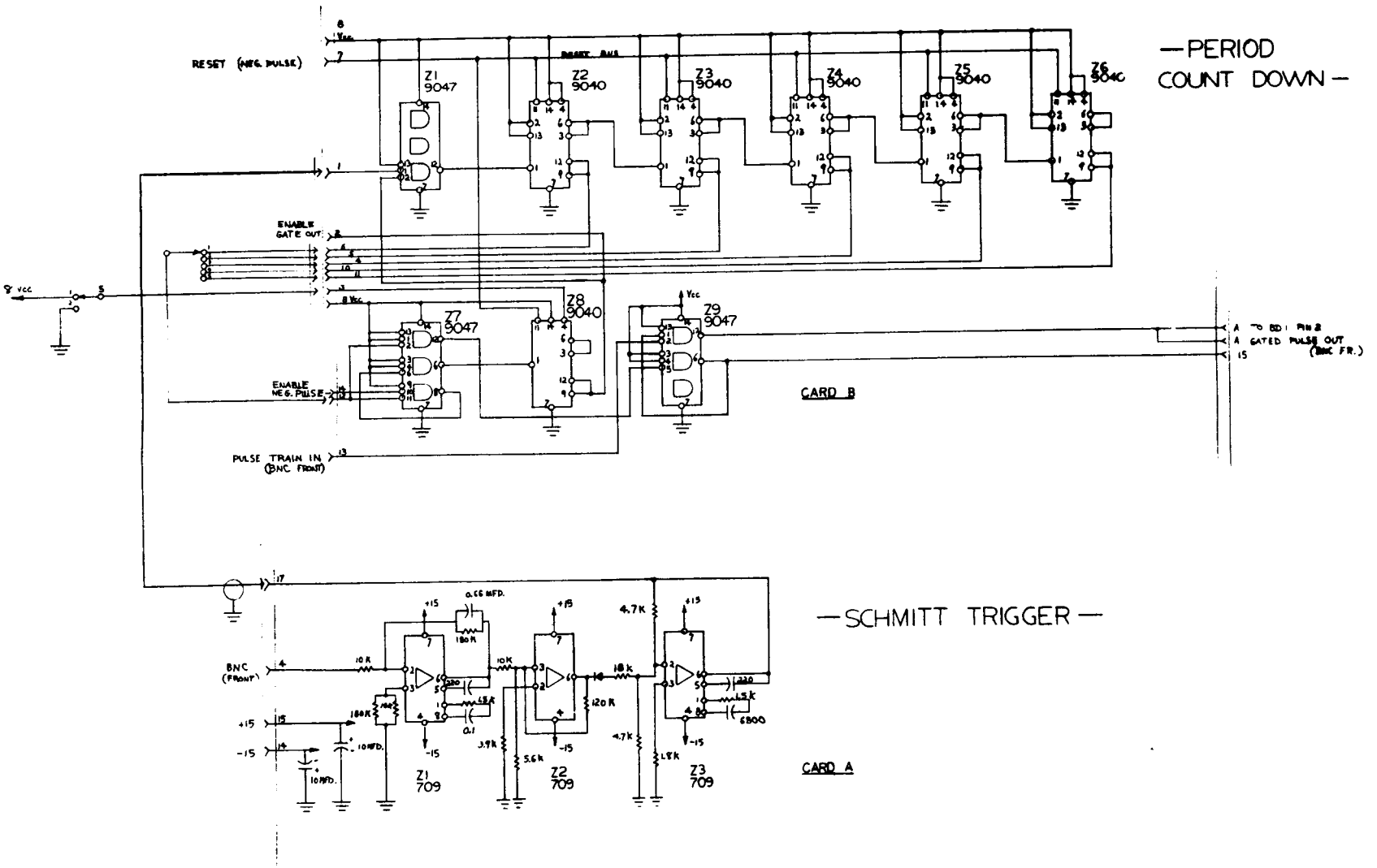

The period pulse, one, two, four, eight or sixteen input periods long as selected by a switch, is returned to gates Z7 and Z9. The period pulse opens the upper gate of Z9, permitting the 100 Hz pulse train to pass through to the reversible counter. The trailing edge of the period pulse resets flip-flop Z8 which in turn closes gate Z1, ending the period measurement until another enabling pulse is received.

Reversible Counter and Jam Transfer Buffer-- The fifteen stage reversible binary counter is shown schematically in Figures B-12, B-13 and B-14. The counting J-K flip-flops Z2, Z4, Z6, Z8 and Z10 on Cards 1 and 2 and Z2, Z4, Z8 and Z10 on Card 3 are initially cleared to zero. Z6 on Card 3 is set to one so that the binary number 001000000000000 is preset into the counter.

Initially, the counter is set to count "up." A set pulse is applied to the "up pulse" input of R-S flip-flop, Z17, on Card 1, raising the "down" bus and lowering the "up" bus. The operation of the counter can be understood by examination of stages 15 and 14 on Card 1; all other stages operate in similar fashion. Regardless of the state of Z17, Z2 in stage 15 toggles each time a pulse of the gated pulse train is coupled to the clock input (pin 1) through buffer Z1. Counting "up," the Q output of stage 15 is coupled to Z4 in stage 14 through gate Z3. Thus, when stage 15 makes a transition from 1 to 0, stage 14 will change state. Similarly, each J-K flip-flop in the chain will toggle when the previous stage makes a 1 to 0 transition. At the completion of the "up" count the binary number in the register will be the preset number plus the number of pulses received from the period gate generator (100 T, where T is the length of the period pulse in seconds).

The counter is set to count down by applying a pulse to the "down pulse" input of flip-flop Z17. Z1 continues to toggle at each input pulse. However, the clock input of Z3 is now coupled to the $\overline{Q}$ output of Z1 through gate Z3. Flip-flop Z3 will toggle only when stage 15 makes a 0 to 1 transition. In a similar fashion, each flip-flop in the counter will toggle when the previous stage changes state from 0 to 1.

If we let N equal the number preset into the counter, T_1 be the length of the period pulse during the "down" counting phase, the resultant number in

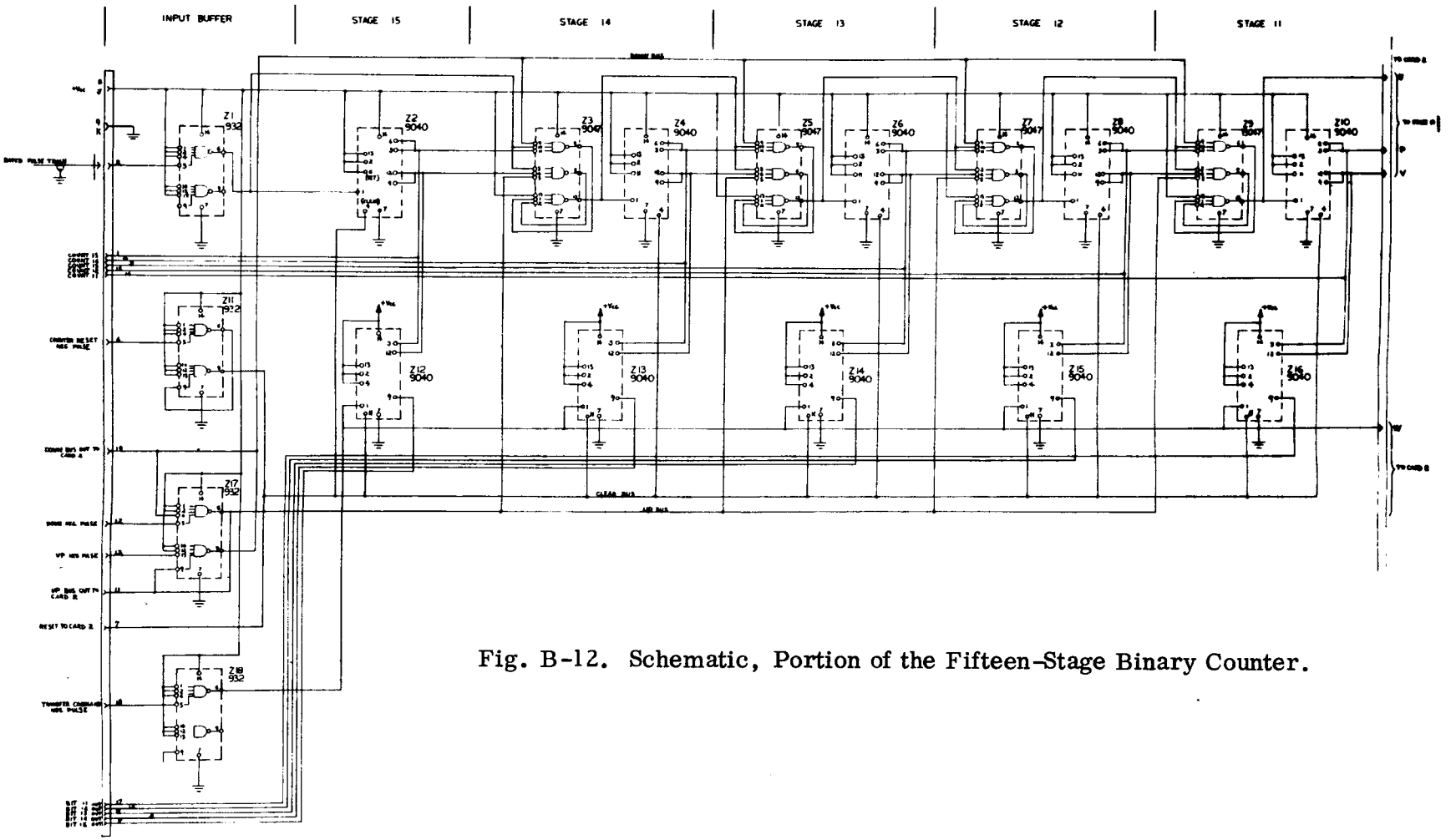

Fig. B-12. Schematic, Portion of the Fifteen-Stage Binary Counter.

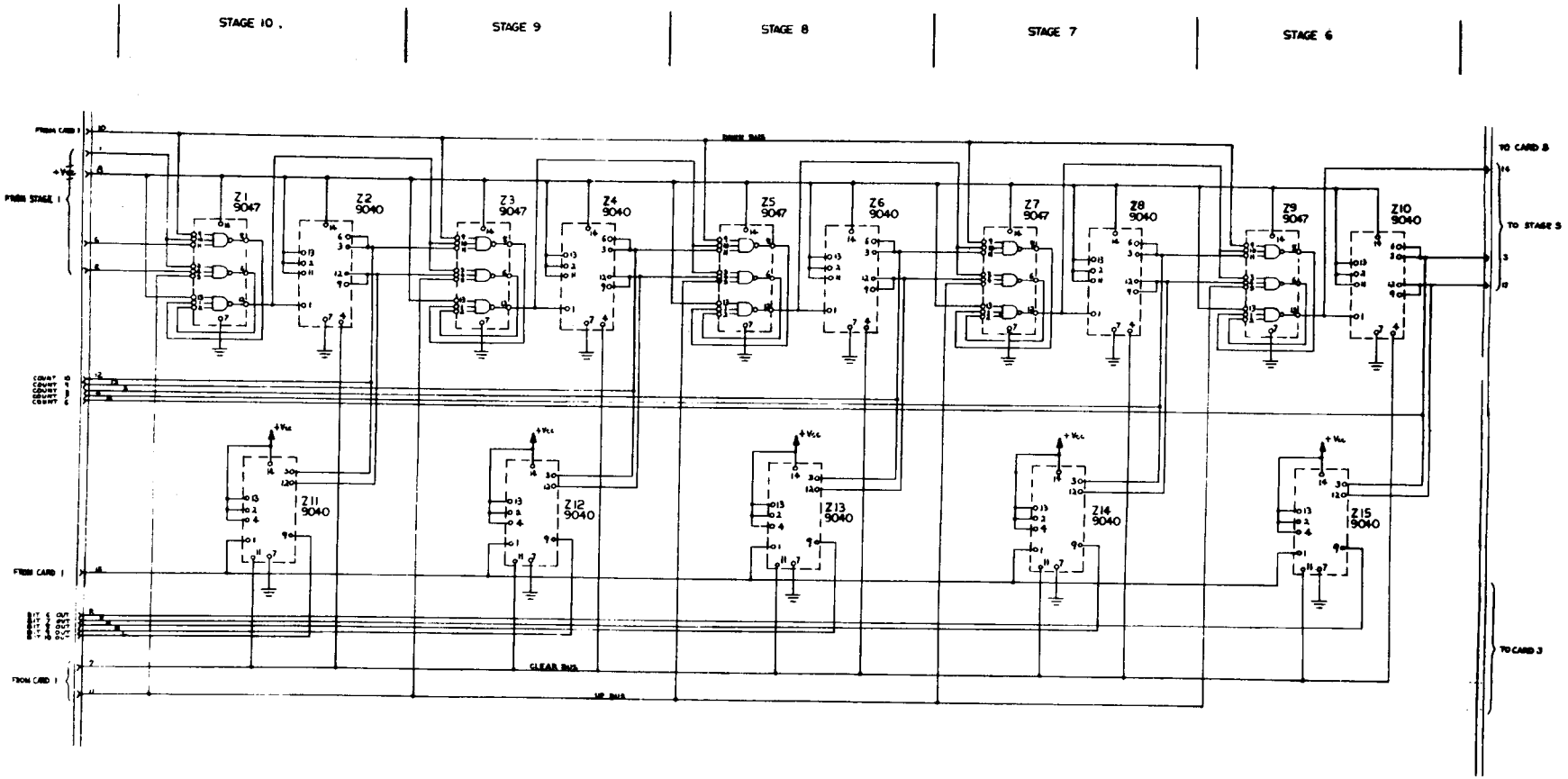

Fig. B-13. Schematic, Portion of the Fifteen-Stage Binary Counter.

Fig. B-14. Schematic, Portion of the Fifteen-State Binary Counter.

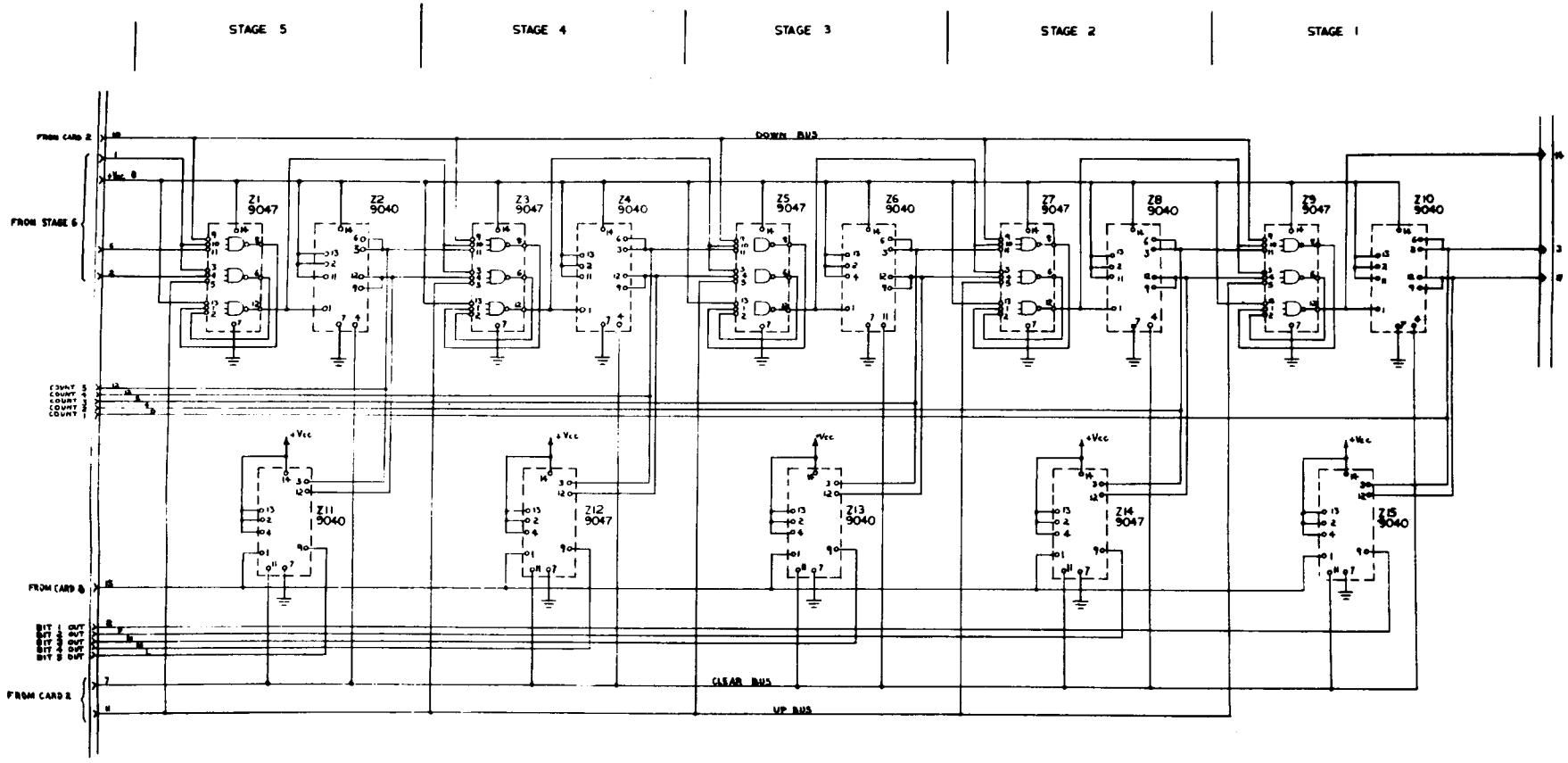

the counter at the end of a complete tuning cycle is

$$N_R = N + 100\ (T_1 - T_2)$$

The pulse train rate and the preset number N have been selected so that N_R is always positive.

At the completion of a tuning cycle, a transfer command shifts the residue number N_R, in parallel, into the jam transfer register composed of flip-flops Z12, Z13, Z14, Z15 and Z16 on Card 1, and Z11, Z12, Z13, Z14 and Z15 on Cards 2 and 3. However, it should be noted that the residue number remains in the counter; the counter is not reset once the tuning cycle begins. The counter performs a digital integration function which is essential to the proper operation of the servo system.

Digital-to-Analog Converter-- The jam transfer buffers furnish the inputs to the twelve-bit digital-to-analog converter shown schematically in Figure B-15. The amplifier transistors, Q1 through Z12, drive the ladder switches Z13, Z14 and Z15. The ladder switches in turn feed the integrated output amplifier, Z19, through the resistor weighting networks Z16, Z17 and Z18. The ladder switches and weighting networks are hybrid microcircuits manufactured by Sprague Electric; the total error in twelve bits is guaranteed to be less than $\pm 1/2$ bit over the full military temperature range. The inset in Figure B-15 shows the circuit configuration of a typical D-A converter stage.

It should be noted that stage 3 is initially preset to one, so that the output of the D-A converter is 5.0 volts (nominal) before the tuning cycle begins. If the residue number in the counter is less than the preset number, the output voltage, after the transfer command is applied, will decrease to less than 5.0 volts. If the residue is greater than the preset, the output voltage will be increased. This technique completely eliminates the earlier problems of polarity sensing and polarity command switching as well as simplifying the reversible counter.

A manual input to the output amplifier is provided so that an external bias voltage can be applied to the varactor.

Fig. B-15. Twelve-Bit Digital-to-Analog Converter.

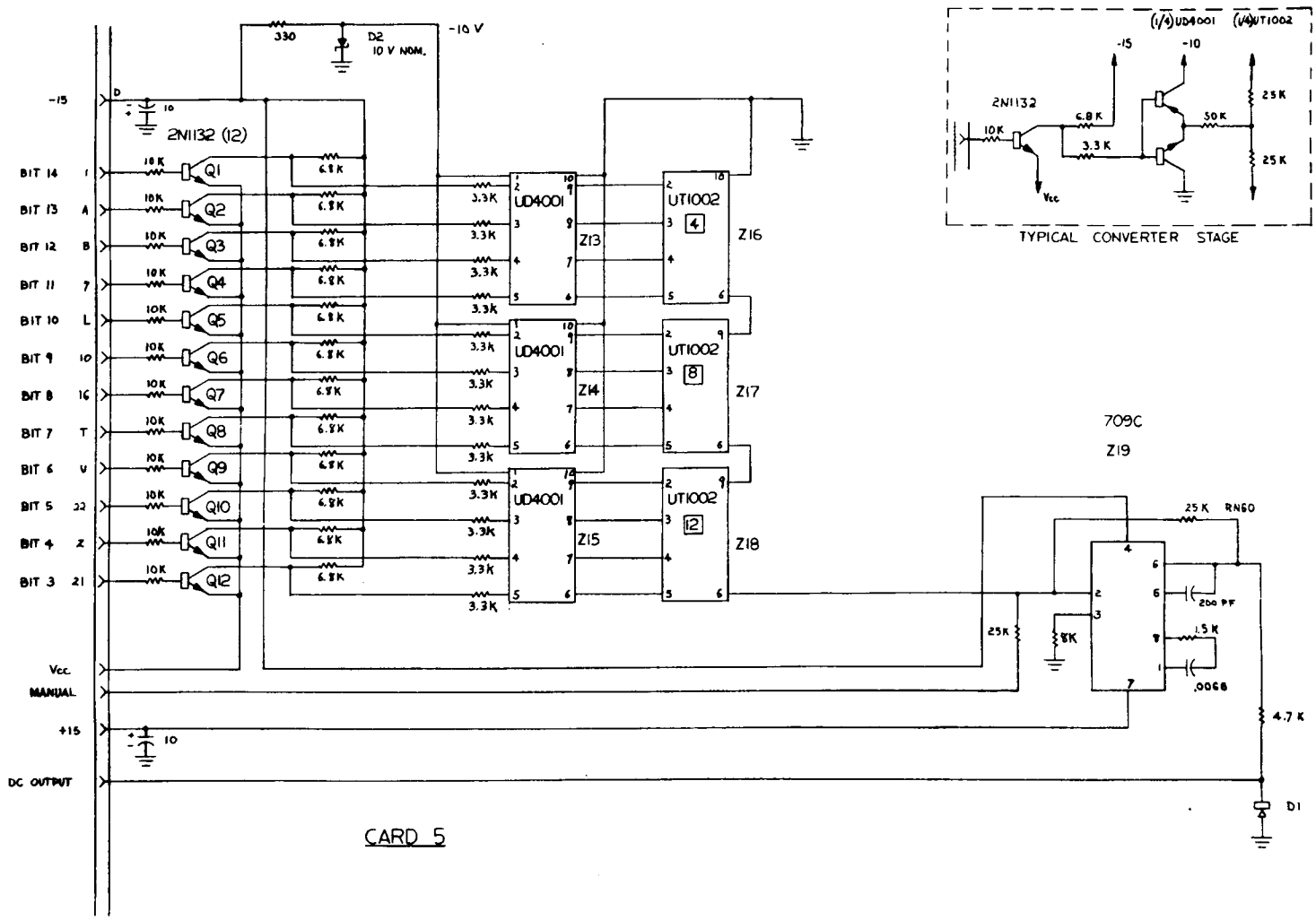

7. Construction--Binary Breadboard

The six printed circuits cards which carry all of the electronics for the tuning computer are shown in the photograph, Figure B-16. The first two cards on the left are the period gate generator, the next three cards hold the fifteen-stage reversible counter and the jam transfer buffers, and the last card is the twelve-bit D-A converter.

Total power requirements are as follows:

+ 15 volts	7.0 ma
- 15 volts	55.0 ma
+ 5 volts	150.0 ma

The computer power dissipation is 1.65 watts total.

Estimated volume and weight for the final, flyable model is approximately 50 $in.^3$ and one pound.

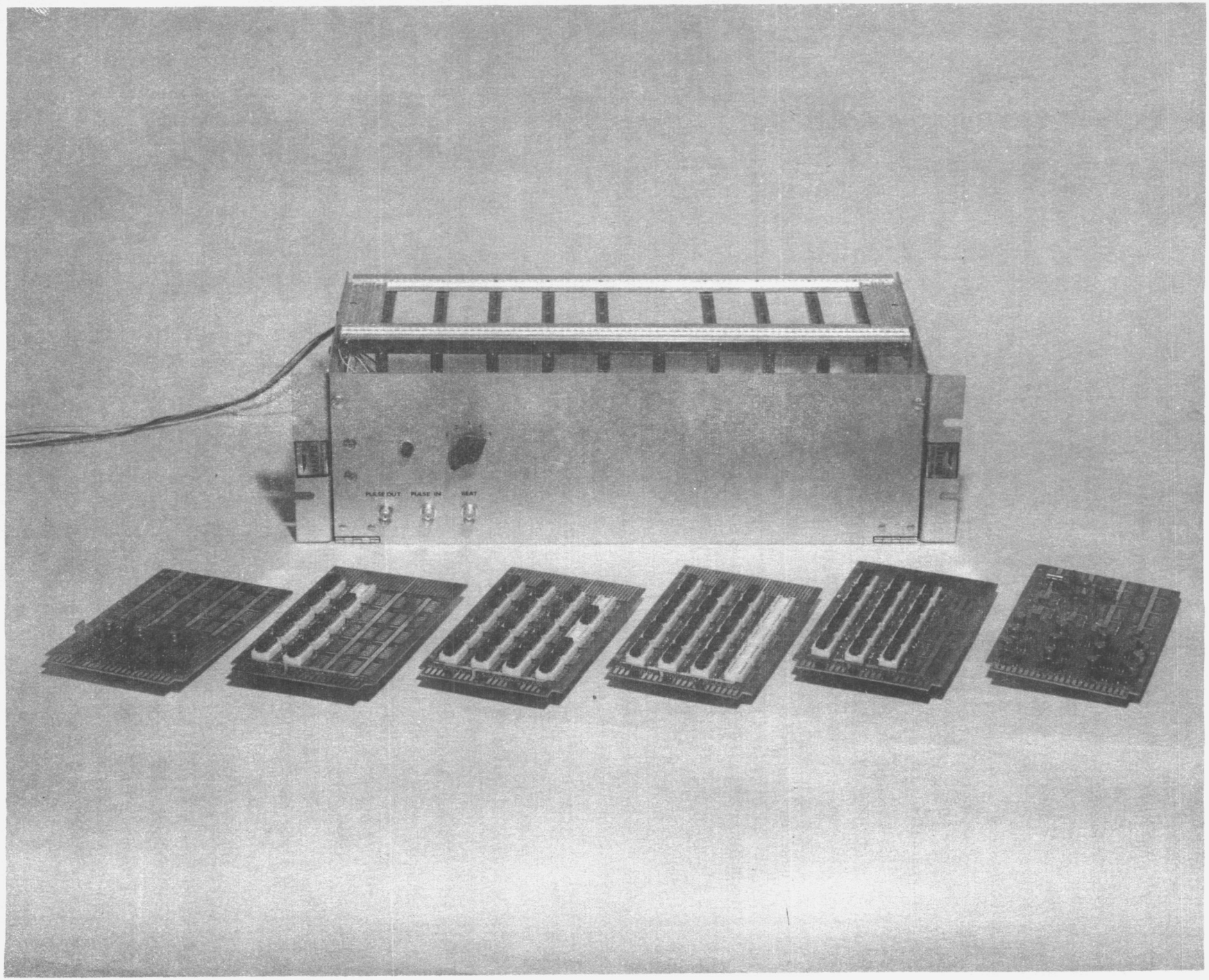

Fig. B-16. Printed Circuit Cards for Tuning Computer.

V. CONCLUSION

The first phase of the contract has successfully demonstrated that a small, lighter weight maser can be made to operate without compromising accuracy or stability. A breadboard prototype electronic system for both tuning the masers and providing useful output signals has been built and has been successfully, continuously operated for a period of nearly a year. The accuracy of tuning, using this method, is within the originally specified goal of 1 part in 10^{13}.

Work on the theoretical aspects of the experiment has continued and an analysis of a doppler canceling telemetry system has been made including the effects of second order doppler shift and gravitational shift. The output information from this system is a direct measurement of the second order doppler and gravitational frequency shift. The accuracy of the experiment is not limited by the telemetry system but depends on the accuracy of the maser oscillator. It is not inconceivable that a tenfold improvement over the original specification can be obtained.

New techniques for stabilizing the oscillator frequency stability will be employed in the future phases of this work. Among these are the use of improved wall coating materials and procedures, the use of low expansion materials such as CER-VIT for the cavity structure, and ultra-high thermal conductivity structures employing the "heat-pipe" principle for removing thermal gradients.

VI. NEW TECHNOLOGY

During the course of the contract some new ideas and techniques were developed. They are as follows:

1. A binary form of the automatic tuner system was developed.

2. A doppler canceling telemetry system was conceived that will permit the measurement of the rate of the satellite clock in terms of the rate of the ground clock in the frame of reference of the ground clock; the system also allows the comparison to be made in the satellite frame of reference. Both sets of data are used so as to eliminate errors due to the possibility of having different propagation velocities to and from the satellite during the frequency comparisons.

3. An improved mechanical design of the r.f. cavity and storage bulb structure has been developed.

4. An improved palladium valve has been designed that has a faster response time and is more easily and reliably fabricated. This design is shown in Figure 6.

5. A compact and lighter weight vacuum pump using the Penning discharge principle was built. This pump has the same capacity for hydrogen consumption as other pumps that are almost twice as heavy.

6. A short beam geometry for focussing atoms in the desired state into the maser storage bulb was devised. The design uses a stopping disc at the exit of the hexapole magnet to prevent particles from the source other than atomic hydrogen in the desired states from entering the bulb.